THESIS FOR THE DEGREE OF LICENTIATE OF ENGINEERING

Packed-Fluidized Bed Reactors – Batch Experiments and Fundamental Modeling with Random Metal Packings

NASRIN NEMATI

Department of Space, Earth and Environment

CHALMERS UNIVERSITY OF TECHNOLOGY

Gothenburg, Sweden 2022

Packed-Fluidized Bed Reactors – Batch Experiments and Fundamental Modeling with Random Metal Packings

NASRIN NEMATI

Department of Space, Earth and Environment
Division of Energy Technology
Chalmers University of Technology
SE-412 96 Gothenburg
Sweden

Printed by Chalmers Reproservice
Gothenburg, Sweden 2022

Packed-Fluidized Bed Reactors – Batch Experiments and Fundamental Modeling with Random Metal Packings

NASRIN NEMATI

Department of Space, Earth and Environment

Chalmers University of Technology

Abstract

The aim of this work is to investigate the effect of random packings on heat and mass transfer phenomena, when applied in bubbling fluidized beds. For this purpose, first, the heat transfer coefficient to a horizontal tube submerged in a fluidized bed containing various types of random packings was investigated. Then, the conversion of different gaseous fuels during chemical-looping combustion (CLC) was studied in packed fluidized reactors with selected random packings. The experimental set-ups consisted of cylindrical laboratory-scale bubbling fluidized-bed reactors with an inner diameter of 78 mm and a height of 1.27 m.

For the first set of experiments, a horizontal tube (d_o=6 mm), through which there was a flow of water, was submerged in the bed. Air was used as fluidizing gas. Silica sand in the size range of 212-300 µm was used as bed material. Heat transfer coefficient, pressure drop and vertical segregation of solids were evaluated experimentally for bed temperatures ranging from 400 °C to 900 °C and superficial gas velocities from 0.04 m/s to 0.411 m/s. The bed height was 13 cm at rest for experiments, with and without packings. Five different types of packings were evaluated for the heat transfer experiments: i) RMSR (25 mm stainless steel thread saddle ring), ii) Hiflow (25 mm stainless steel pall ring), iii) RR6 (6 mm ceramic Raschig ring), iv) RR10 (10 mm ceramic Raschig ring) and v) ASB (12.7 mm aluminum silicate balls). For the second set of experiments, three of the packings (ASB, RMSR and Hiflow) were selected. CLC experiments were conducted using three fuels: CH_4, CO and syngas (50/50% H_2/CO), at temperatures between 840-940°C.

The results show that the nature of the packings has significant impact on the behavior of a packed-fluidized bed. Packings with low void factor such as RR6, RR10 and ASB had lower heat transfer coefficient, higher pressure drop and more significant vertical segregation, compared to a bubbling bed without packings. Packings with high void factor were quite different. The RMSR packing showed an improvement in heat transfer coefficient (up to 1243 W/m^2K) at higher gas velocities, as compared to bubbling bed with no packings (up to 1124 W/m^2K). Also, beds with RMSR and Hiflow packings had lower pressure drop, lower vertical segregation and higher fuel conversion in CLC compared to a bubbling bed with no packings.

It is concluded that packings with high void factor such as RMSR and Hiflow can be used in bubbling fluidized bed with small impact on pressure drop and solids segregation, and potentially positive effect on both heat and mass transfer. Packings with low void factor may be of interests for other applications, which remains to be explored.

Keywords: Bubbling fluidized bed, Chemical-looping combustion, Random packing, Packed-fluidized bed, Mass transfer, Heat transfer, Confined fluidization.

List of publications

The thesis is based on the following appended papers, which are referred to in the text by their assigned Roman numerals:

I. Nemati N., Andersson P., Stenberg V., Rydén M., Experimental Investigation of the Effect of Random Packings on Heat Transfer and Particle Segregation in Packed-Fluidized Bed. *Industrial & Engineering Chemistry Research 2021;* **60:** 10365-10375. DOI: 10.1021/acs.iecr.1c01221

II. Nemati N., Rydén M., Chemical-Looping Combustion in Packed-Fluidized Beds: Experiments with Random Packings in Bubbling Bed. *Fuel Processing Technology 2021;* **222:** 106978. DOI: 10.1016/j.fuproc.2021.106978

III. Nemati N., Tsuji Y., Mattisson T., Rydén M., Chemical-Looping Combustion in Packed-Fluidized Bed Reactor – Fundamental Modeling and Batch Experiments with Random Metal Packings. *Accepted for publication in Energy & Fuels 2022.*

Nasrin Nemati is the principal author of **Papers I**, **II** and **III**, and conducted most of the work for these papers. Magnus Rydén contributed with conceptualization, modeling, review, editing and discussion of all the papers. Tobias Mattisson contributed with modeling, review, editing and discussion of **Paper III**. Pontus Andersson and Viktor Stenberg contributed with the experiments of **Paper I**. Yukari Tsuji contributed with the experiments of **Paper III**.

Other publications

Other publications by the author, not included in the thesis:

A. Nemati N., Moreno P.F., Rydén M., Investigation of the Hydrodynamics of Packed-Fluidized Beds: Characterization of Solids Flux, The 24th International Conference on *Fluidized Bed Conversion, Göteborg, Sweden, 2022* (Accepted).

Acknowledgements

Firstly, I would like to thank my supervisor Magnus Rydén and my co-supervisors David Pallarès and Tobias Mattisson for the opportunity to pursue my PhD with your support. Special thanks to Magnus, for all your help and guidance during these years. You have always provided me a pleasant environment to study and work in and have helped me anytime I needed it. I would always appreciate your support and guidance whenever I saw an obstacle on the way of my PhD journey.

I would like to acknowledge the Swedish Energy Agency (project 46525-1 - The application of confined fluidization in energy conversion) for the financial support of my work.

I would like to thank my wonderful colleagues in the CLC and fluidization groups for the interesting discussions in both formal and informal meetings as well, for all the good teamwork and the joy of not working alone. Also, thanks to everyone at the division for making Energy technology such a nice and wonderful working place. All the division activities, seminars, games, after-works, Friday fikas and gatherings that we did all together are having a special place in my heart. Thinking about them always bring a smile on my lips and warms my heart. I also want to thank Viktor Walter for the great years of office sharing with all the discussions and helps about everything even during pandemic and his parental leave. Thanks to Rustan Hvitt for his great help in building-up my new set-up. Looking forward for many interesting results in the new cold-flow model in the future.

Finally, Many thanks to my family: my mother, father, and my sisters. You have always supported me and believed in me from the beginning. Thanks for everything. Andreas, thank you for your support on this journey and beyond; I can't wait for all of our future adventures together.

Nasrin Nemati
Johanneberg, May 2022

Table of Content

1 Introduction

A goal to restrict global warming to well below 2°C above pre-industrial levels, was agreed upon in Paris in 2015 [1]. To meet this target, rapid decarbonisation of all energy sectors is needed, together with large-scale deployment of negative-emissions technologies [2]. Carbon capture and storage (CCS) is a set of technologies that could reduce CO_2 emissions from point sources such as fossil power plants and industrial facilities. The viability of different CO_2 separation concepts has been recognized for many years. Therefore, many CCS projects utilizing technologies such as for example amine scrubbing and oxy-fuel combustion have been launched all over the world in the past decades [3]. Each technology evaluated has strengths and weaknesses in terms of cost, efficiency, and applicability [4].

Among different CCS technologies, chemical looping combustion (CLC) is recognized for its potential to capture CO_2 at relatively low cost and with high efficiency [5]. In a conventional combustion facility, fuel burns by mixing it with ambient air. Thus, the flue gas consists mainly of nitrogen, in mixture with excess oxygen and the combustion products H_2O and CO_2. The low CO_2 partial pressure in the flue gas makes CO_2 separation after conventional combustion a complex and expensive process. However, CLC does not have the nitrogen dilution problem. This is because fuel is oxidized with solid metal oxide oxygen carriers instead of air [5].

Most often, CLC utilizes fluidized-bed reactors. In such reactors it is important to achieve high and uniform gas-solid mass and heat transfer, as this will enhance gas conversion. Fluidization was established as an industrially important concept in the 1940's, during which large scale implementation of fluid catalytic cracking was introduced. Advantages of fluidized bed reactors include very good heat and mass transfer rates, excellent gas-solid contacting and temperature uniformity [6]. It soon extended its range of applications to other areas such as heat transfer, coating, drying, combustion, gasification, chemical reactors and adsorption [6–9].

Fluidization is a phenomenon in which solid particles are transformed into a fluidlike state, through suspension in a gas or liquid [6]. Figure 1 shows different regimes of fluid-solid contact, established by increasing the fluid velocity from left to right. When a fluid passes upward in a bed of particles, if the flow rate is very low, the fluid just permeates through the voids between stationary bed particles. This is referred to as a fixed-bed reactor. By increasing the flow rate, a point is reached where all the particles are suspended by the fluid. The superficial gas velocity at this point is referred to as minimum fluidization velocity. At this velocity the friction force between particle and fluid is equal to the weight of the particles, the vertical component of the compressive force between adjacent particles disappears. Thus, the pressure drop throughout the bed equals the weight of fluid and particles inside the bed. Further increase in the fluid velocity beyond minimum fluidization results in formation of gas bubbles and sometimes with channeling occurring inside the bed. This is referred to as a bubbling-fluidized bed. For deep beds in narrow columns, bubbles' diameter can become as large as the

cross section of the vessel. This mode of operation is called slugging and should typically be avoided in practical applications. At even higher gas velocities, terminal velocity of solids is exceeded, meaning that particles will be transferred upwards by the fluid flow. Depending on process conditions, turbulent fluidization or pneumatic transport of solid will occur eventually [6].

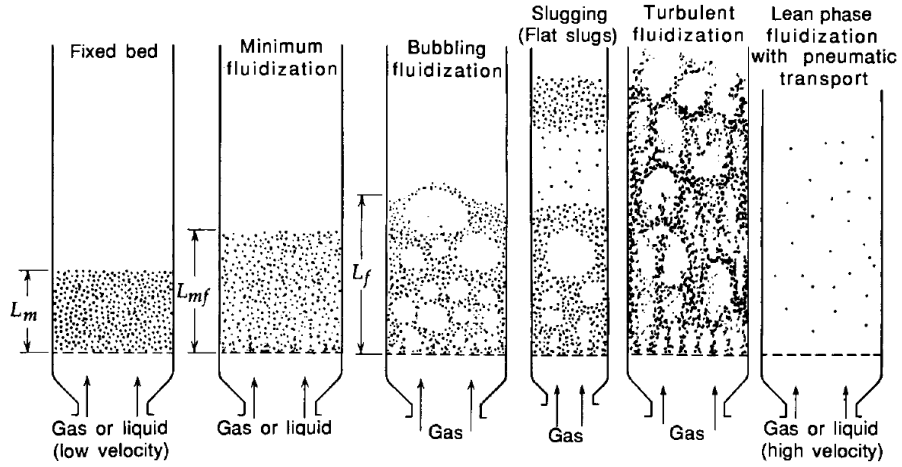

Figure 1:Illustration of fluidization regimes, by increasing the fluid velocity from left to right.

One challenging issue with fluidized bed reactors is the potential for reduced gas-solid mass and heat transfer at higher superficial gas velocities, especially when deep beds are used. This could occur due to bubble growth. It is easily realized that large bubbles result in reduced contact between gases and solids, which is necessary to achieve high gas-solid mass transfer and high heat transfer. Bubble growth could also lead to other undesirable fluidization phenomena such as slugging. These factors are critical to technologies such as chemical-looping combustion (CLC). For example, in bubbling bed CLC with the most commonly used bed materials, the only chance for fuel oxidation in the fuel reactor will be within the bed. This eliminates the possibility of fuel conversion in the freeboard due to exclusion of oxygen carrier in this section. If undesired phenomena such as slugging, channeling and bubble growth occurs, the fuel conversion and efficiency will decrease drastically. Here, the role of packed-fluidized beds in avoiding these phenomena is distinguished.

Various methods for overcoming the restriction mentioned above and improving the quality of gas-solid fluidization have been proposed. These solutions range from adding mechanical constructions such as disks, trays and concentric mesh screens, to movable packings such as glass beads, Berl saddles and Raschig Rings. The purpose of such devices is to break down large bubbles formed inside the bed to smaller ones [10], [11].The use of fixed parts involves several problems. This includes erosion, difficulties to replace worn-out parts and potentially mechanical stress for operation at elevated temperature. Therefore, the idea to apply random packings in fluidized bed reactors to prevent bubble growth in applications such as CLC could potentially be of importance.

Therefore, the idea to apply random packings in fluidized bed reactors to prevent bubble growth in chemical-looping combustion has recently been suggested [12]. The concept of using random packings in fluidized beds is referred to as packed-fluidized bed or confined fluidization. Random packings are used in many different chemical and thermal processes and

are available in many shapes, sizes, forms and materials. In general, in chemical processes, a packed bed is a vessel that is filled with a packing material. As illustrated in Figure 2, a device or reactor can be filled with small objects like raschig rings, pall rings, saddle rings etc. (random packing) or with a specifically designed structured packing (structured packing).

a) b)

Figure 2: Packing types in packed beds: a) random packing, b) structured packing.

Packing material can be used instead of trays to improve separation e.g., in distillation columns. Packing offers the advantage of a lower pressure drop across the column (when compared to plates or trays), which is beneficial. Also, as mentioned above, other issues such as erosion and mechanical stresses can be avoided by applying the random arrangement. Structured packing compared to random packing usually has lower pressure drop but it is more expensive. Differently shaped packing materials are characterized by their different surface areas and void factors. Both of these parameters affect performance.

The void factor is a measure of the empty spaces in the packing. The void factor is a fraction of the volume of voids over the total volume, when packings are applied to a vessel. Using this definition, it will vary between 0 and 1. There are many ways to evaluate the void factor. One of these methods can be done through a simple set of experiments. To find the void factor of packing materials, an empty container can be filled with water and weighed. The container can then be emptied and filled with packings. Water will be added into the packed container until it is completely full and weighed. Dividing the weight of the water in the packed container by the weight of the water in the unpacked container, gives the void factor. A high void factor indicates much empty space between packings. Thus, the fluid can flow easily through the packed zone. In general, in a high void packing, flow capacity is increased, and pressure drop is decreased, as compared to packings with low void factor.

1.1 Aim and scope

This thesis focuses on examining:

(i) how different types of random packings will affect the heat transfer rate, pressure drop and particle segregation in a bubbling fluidized bed at elevated temperature.
(ii) how random packings will impact fuel conversion rate in CLC.
(iii) how to model the bubble size and gas interchange coefficient in the bed containing packings.

The ultimate goal of the work is to show that use of random packings is a viable method to significantly improve performance in future applications of fluidized-bed reactors, especially chemical-looping combustion (CLC).

1.2 Contribution of this thesis

This work contributes to understanding the above questions and address them in the appended papers. Figure 3 shows an overview of the appended papers and their main contribution to the investigations. In **Paper I**, the effect of five different types of random packings on heat transfer rate in bubbling fluidized bed were investigated. The studied packings were:

- 25 mm stainless steel thread saddle ring RMSR 25-3 (RMSR)
- 25 mm stainless steel pall ring Hiflow 25-5 (Hiflow)
- 12.7 mm aluminum silicate balls (ASB)
- 6 mm ceramic Raschig ring (RR6)
- 10 mm ceramic Raschig ring (RR10)

The main difference between these packings is their structure, void factor, material and bulk density. RMSR and Hiflow can be categorized as being high void packings (void factor > 0.95), as compared to the others (with void factor < 0.6). **Paper I** also investigate the effect of above packings on pressure drop and vertical segregation of fluidizing solids. In **Papers II** and **III**, different selections of packings are considered from the above list and subjected to analysis in CLC batch experiments. **Paper II** compares two different fuels (CO and CH_4) in the beds containing following packings. Then the results are benchmarked against bubbling beds without packings.

- 25 mm stainless steel thread saddle ring RMSR 25-3 (RMSR)
- 12.7 mm aluminum silicate balls (ASB)

In **Paper III**, the CO and syngas (50/50% H_2/CO) fuels conversions are compared for the beds containing the below highly evolved packings:

- 25 mm stainless steel thread saddle ring RMSR 25-3 (RMSR)
- 25 mm stainless steel pall ring Hiflow 25-5 (Hiflow)

Additionally, a model will be introduced in **Paper III** to evaluate the impact of packings on the bubble size and gas interchange coefficient in the bed.

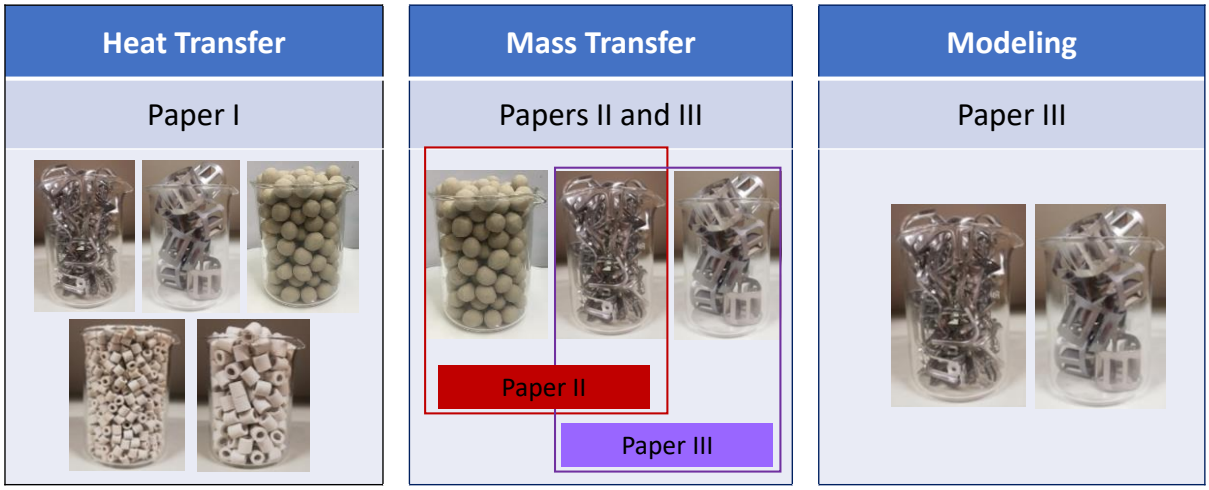

Figure 3: Thesis structure. Overview of the appended papers and their main contribution to the investigations.

2 Background

According to Abrahamsen and Geldart [13], the two most important particle properties that affect the fluidization characteristic of a fluidized bed are the particle size and particle density. Thus, particles are commonly characterized based on these two properties. Geldart divided different particulate materials into four main groups based on their density, diameter, their different flow regimes and fluidization characteristics [14], [15]. Among these groups, Geldart group B with bulk density from 1400 kg/m^3 to 4000 kg/m^3 and size range of 40 µm to 500 µm has proven to be very useful in industrial applications, such as for example combustion and gasification [16–18].

Group B particles do not tend to undergo smooth fluidization. Rather, bubbles form already at the onset of fluidization. For Geldart group B, the bubble size becomes larger as the bed height and gas velocity increases. Thus, group B particles tends to allow the formation of very large bubbles. Therefore, slugging can occur even in bigger units. Another challenging issue with fluidized bed reactors using group B particles is the potential reduction of gas-solid mass transfer at high superficial gas velocities, especially in deep beds. This is due to bubble growth and bubble coalescence. Small bubbles in a bubbling fluidization are desirable for effective mass transfer, but larger bubbles reduce the contact between gases and solids, which most often is undesirable. Specifically for the case CLC, where deep beds are often strived for, in a fuel reactor containing Geldart group B particles bubbles could coalescence and grow. Bubbles growth can continue until they cover the reactor cross section, resulting in phenomena such as slugging and channeling and poor fuel conversion [19–23].

2.1 Chemical-looping combustion (CLC)

Chemical-Looping-Combustion (CLC) is a promising technology for generation of heat and power with inherent CO_2 capture. The broader chemical-looping concept also has other potentially important applications such as combustion, gasification, reforming, and hydrogen production [24–27]. Here, the focus will be on the combustion application.

CLC utilize solid metal oxide particles and a setup with two interconnected reactors, typically referred to as the Air Reactor (AR) and Fuel Reactor (FR), see Figure 4.

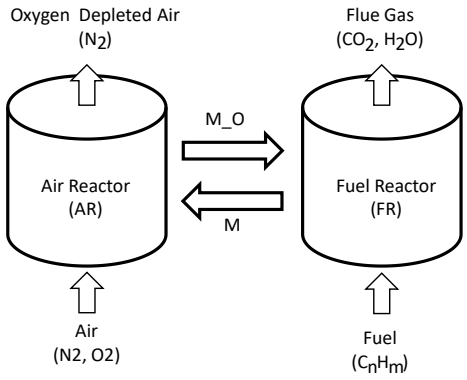

Figure 4: Schematic description of Chemical-Looping Combustion (CLC).

In the fuel reactor, the oxygen carrier particles are reduced by the fuel (C_nH_m), which in turn is oxidized to CO_2 and H_2O. In the air reactor, the particles are oxidized with O_2 from air. The reactor temperature is typically in the range 800-1000 °C. An example of the reactions in each reactor vessel and for the system as a whole can be found in reactions (1-2) below, where M_O represents the oxidized oxygen carrier and M the reduced oxygen carrier.

$$C_nH_m + \left(2n + {}^1/_2\, m\right) M\_O \rightarrow nCO_2 + {}^1/_2\, mH_2O + \left(2n + {}^1/_2\, m\right) M \quad (1)$$

$$M + {}^1/_2\, O_2 \rightarrow M\_O \quad (2)$$

The main advantage of CLC is that it prevents dilution of flue gases with air. Essentially pure CO_2 can be obtained by cooling the fuel reactor gas, condensing steam to water. If used for CO_2 capture, CLC eliminates the need for a separate and costly gas separation step [28–31]. The reactors in the CLC process can be designed using different principles, such as bubbling fluidized bed, circulating fluidized bed, fast fluidized bed, moving bed or fixed bed [32–36]. Among the alternatives, two interconnected fluidized bed reactors present clear advantages such as good temperature control and steady flow of oxygen carrier particles between the air reactor and fuel reactor. This is also the design most commonly envisioned in literature.

2.2 Packed-fluidized bed

A conventional bubbling-fluidized bed (BFB) can be divided into two main phases: the bubble phase or the diluted phase, which is mainly the fluidizing gas in the form of bubbles, and the emulsion phase or the dense phase, which mainly consists of bed particles (Figure 5a). Previous studies showed that in a BFB, the mass transfer rate of gas between bubble and emulsion phase decreases with an increase in bubble size [12], [37–39]. While small bubbles are desirable for effective mass transfer, large bubbles can have the opposite effect by causing gas bypass and slugging [23]. One effective method to eliminate bubble growth in BFB is applying the concept of packed-fluidized beds [11], [12], [40]. In this method, inert stagnant packings of much larger size than the fluidized particles are applied to breakdown the larger bubbles, as illustrated in Figure 5b.

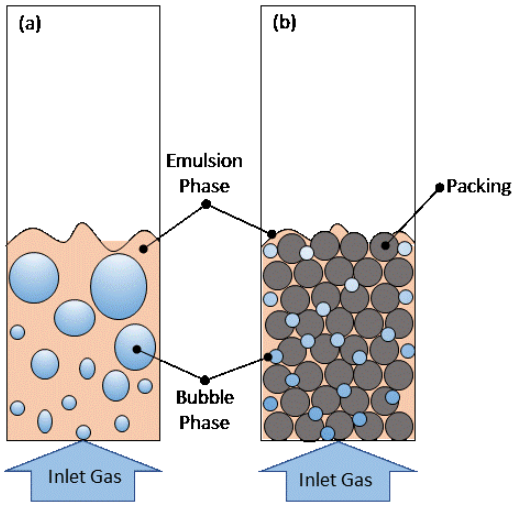

Figure 5: Illustration of a) conventional BFB, b) packed-fluidized bed.

Packed-fluidized beds have not been extensively studied. That said, some studies about the use of packed-fluidized beds for various applications has been presented in the literature, examining for example heat transfer [41–43], axial dispersion [44], bed expansion [45], [46], and hydrodynamic behavior of gas-solid beds [44], [47]. The effect of packings on fluidization was first investigated by Gabor and Mecham [48] and Sutherland et al. [11], who investigated the effect of spherical packings on hydrodynamics and heat transfer rates in fluidized beds. They documented fundamental fluidization properties and observed that a combination of packed beds and fluidized beds can improve the heat transfer rate. A few studies on packed-fluidized beds have been done afterwards about topics such as catalytic reactions [49–52] and hydrodynamic properties such as minimum fluidization properties and pressure drop [40], [47], [53]. Donsi et al. [45] and Girimonte et al. [46] studied the expansion behavior of fine particles in a packed bed of spherical coarse particles at room temperature, in the velocity range up to 10 times the minimum fluidization velocity. Both research groups presented models for the bed expansion behavior of particles in a packed-fluidized bed, based on experimental results. The models describe hydrodynamic properties such as pressure drop, minimum fluidization velocity and bed voidage. In other works, Girimonte et al. [54], [55] investigated CO_2 adsorption on zeolite pellets in a packed-fluidized bed using glass spheres as packings. They observed that, for a given mass of sorbents, CO_2 adsorption increased compared to fixed beds, because of suppression of bubbles growth.

Recently, Aronsson et al. [12] successfully applied spherical packings in CLC batch experiments and found improved fuel conversion rates compared to a conventional bubbling fluidized bed. However, there are no studies on other forms of packings and their effect on fuel conversion in this field of research. Also, the use of spherical packings in a fluidized bed may break down bubbles, but it could also constitute a major hinderance for fluidization. It may also influence factors such as the heat transfer rate significantly compared to non-packed beds [11]. Studies of fluidized-packed beds with evolved packing materials with high void factor and the impact on factors such as mass and heat transfer and particle segregation are currently lacking.

Table 1 summarizes the most important investigations that has been done on packed-fluidized bed concept in the literature.

Table 1: Summary of investigations on packed-fluidized bed concept.

No.	Packing	Bed material	Results	Year	Ref.
1	Fixed stainless-steel strips coated by silver catalyst	Glass beads (inert bed)	- Silver catalyst for oxidation of ethylene to ethylene-oxide was sprayed on stainless steel strips which were attached to a centrally located supporting structure. - This method was examined to avoid agglomeration problem yet obtaining an excellent heat transfer property. - Small scale tests with this method, showed that excellent temperature control could be achieved without serious adverse effects on catalyst performance.	1960	[49]
2	Uniform spheres	Glass beads	- The effect of fixed packing on the properties of a gas-fluidized bed, including minimum fluidization velocity, pressure drop, and bed expansion was studied experimentally. - Experiments indicated that both packing size and the ratio of particle to packing diameter were the main variables in correlating the results. - A preliminary study was also made for heat transfer rates, and the results indicated that with spherical packing, values of heat transfer coefficient were of the order of 70% of that in a conventional bed.	1963	[11]
3	Spheres and cylindrical packing	Glass beads, Aluminum oxide, copper	- Radial gas mixing in the voids of fixed packings was investigated. - Results showed that values of gas eddy diffusivities in the fluidized-packed beds were nearly the same as values in beds with the same type of packing but without the fluidizing materials. - Due to nonuniform pressure gradients associated with fluidization in packings, large variances in the eddy diffusion coefficient was observed compared to non packed beds.	1964	[56]
4	Fixed stainless-steel cylindrical strips	α-Alumina and Glass beads	- Silver catalyst was sprayed on vertically mounted cylindrical strips for the strongly exothermic reaction of ethylene oxidation where the fluidized bed acted as an effective heat transfer medium in removing heat from the catalyst to the wall of the reactor. - They minimized the stagnant regions by this method and provided a good heat transfer from the catalyst surface. - Close temperature control was achieved so long as good fluidization around the packing was maintained. - For glass beads, poor fluidization was observed when sticking developed thus causing a large axial temperature profile.	1964	[50]
5	Spherical and cylindrical packings	Copper and nickel	- The lateral mixing behavior of particles fluidized in the voids of a packed bed is analogous to eddy diffusion in a flowing gas stream. - A model was used to relate the solids diffusivities to the void structure of the packed bed. - A dimensional correlation for solids diffusivity in a spherically packed bed was empirically deduced. - The rate of solids mixing increased with bed height for no packing but was independent of height for fluidized-packed beds.	1964	[57]
6	Spherical packing	Copper and nickel	- A model was developed to relate average particle velocity to the fluidizing gas velocity - A correlation for lateral solids mixing in a packed-fluidized bed was presented from the average particle velocity and the diameter of the fixed packing.	1965	[58]

Table 1(continue): Summary of investigations on packed-fluidized bed concept.

No.	Packing	Bed material	Results	Year	Ref.
7	Steel spheres	Cu-Ni, alumina and glass	- Effective thermal conductivities for lateral heat transfer were measured in a fluidized-packed bed. - A general correlation was made for the fluidized-packed bed thermal diffusivities with the size of the spherical fixed packing and the minimum fluidization velocity.	1965	[59]
8	Cylindrical screen packing (Pall ring)	silica-alumina cracking catalyst	- Effect of packing on the catalytic isomerization of cyclopropane in fixed and fluidized beds were studied. - The effects of various cylindrical screen packing, on final conversion were determined. - Overall conversions were higher in a fluidized bed with packing than in a normal fluidized bed but were less than in a fixed bed. - Rate data from the fixed bed closely followed first-order kinetics. When the same catalyst was tested in a normal fluidized bed, the rate was dependent on linear gas velocity and catalyst bed height. With packing present in the fluidized bed, this dependency was much less, but packing size and shape had some effect.	1965	[51]
9	Cylindrical UO_2 pellets	An inert material	- Fluorination of depleted uranium pellets were studied in this work in a packed- fluidized bed system. - In their proposed system, the uranium pellets would be the packing solids and the fluidizing solids would be used as heat transport medium. - They investigated and formulated expressions for some basic fluidization phenomena such as pressure drop, solids mixing and bed expansion. - It was found that the addition of fluidizing solids increased the heat transfer coefficient by a factor two at the reactor walls, and eight at the top of the packing.	1965	[60]
10	screen cylinders	Sand, Alumina, glass bead, cracking catalyst, polystyrene	- It was shown that a unique relationship between the relative velocity and the bed voidage did not exist. Consequently, simple batch measurements were not sufficient to describe the hydrodynamics of co- or counter-current flows (in contrast to liquid-solid fluidized systems. - A reason for the non-existence of this relationship was attributed to the fact that friction forces between packing and particles greatly contribute to the balance of forces for counter-current and also for batch systems.	1976	[47]
11	Pall rings, Raschig rings and cylindrical screens	Silica-alumina catalyst (Geldart A)	- The hydrodynamic behavior of packed-fluidized beds regarding the gas-solid counter-current operation was investigated. - Pressure drop, hold-up, loading and flooding were evaluated and compared with literature data for gas-liquid systems. - They derived a correlation for the pressure drop, which was mainly caused by suspended particles.	1979	[61]
12	Pall rings	Silica-alumina catalyst (Geldart A)	- The height of an overall mass transfer unit was measured in a gas-solid packed bed by steady state adsorption. -Then the mass transfer and axial dispersion was investigated for adsorption process with an extended model. - They showed that the height of true transfer unit was approximately independent of the solid mass flux and increased with increasing gas velocity. At low gas velocities axial dispersion of the gas and especially of the solid phase was the determining factor for column performance. At higher gas velocities mass transfer limitations became important.	1979	[62]
13	Fixed packing of nickel on alumina catalyst	Alumina and glass beads	- kinetics and mass transfer for catalytic hydrogenation of ethylene in a packed-fluidized bed was investigated. - The mass transfer coefficient and reaction rate constant were evaluated from integral conversion data. - The mass transfer coefficient between the interstitially fluidized bed and the catalyst surface was correlated in dimensionless form.	1979	[52]

Table 1(continue): Summary of investigations on packed-fluidized bed concept.

No.	Packing	Bed material	Results	Year	Ref.
14	Metal tubes	FCC and sand	- The hydrodynamic properties of counter-current gas-solid flow over a regularly stacked packing at trickle flow conditions was studied. - A particle flow model was developed based on the momentum equation of a single particle. - For coarse particles, the maximum gas mass flux at which countercurrent operation was still possible was determined primarily by the local gas velocity in the packing and the terminal velocity of the single particles.	1984	[63]
15	Tubes of square cross-section	Sand	- The heat transfer behavior of a counter-current gas-solid trickle flow contactor was studied. - Experimental data on the overall heat-transfer rate constant between the gas flow and the solid particle flow were obtained experimentally. - Pressure drop over the packings was low, while counter-current heat-transfer properties were remarkable. - Heat transfer behavior was described by a model based on single-particle flow and by incorporating the effect of particle agglomeration at higher solids fluxes.	1986	[41]
16	Ceramic and glass raschig ring and catalyst pellets	FCC	- The pressure gradient and the static and the dynamic hold-up were measured for a system consisting of FCC trickling over a packed bed with a gas streaming in a counter-current flow. - A correlation for the pressure gradient in the preloading region was derived based on the Ergun equation and considering the internal gas recirculation due to the solid's trickles. - A correlation was given which related the boundary between preloading and loading with the particle and gas properties and the solids flow rate.	1987	[64]
17	Coarse spheres	Glass beads, FCC, alumina, copper	- They studied the expansion behavior of fluidized beds of fine particles confined within packings of coarse spheres. - Throughout the whole expansion range, they proposed a general relationship between voidage and gas flow velocities, represented by a two-parameter power law of the Richardson-Zaki.	1989	[45]
18	Coarse spheres	Glass ballotini	- A model based on extension of the Blake-Kozeny equation to binary solid systems was developed to describe confined fluidization of fine particles. - Pressure drop, minimum fluidization velocity and expansion characteristics were determined for the studied bed material.	1990	[65]
19	Spherical elements (porcelain balls)	Sand	- A theoretical analysis based on an extension of the Ergun equation to bi-dispersed granular system was suggested for the correlations determining the minimum fluidization velocity.	1992	[66]
20	Perspex rods	FCC	- The effect of packings on hydrodynamics (pressure drop and solids hold-up) was investigated at ambient conditions, for the riser part of a circulating fluidized bed unit. - They showed that the pressure gradient over the packed section increased linearly with increasing solids mass flux, but faster than linearly with increasing applied gas mass flux. - They presented a correlation to describe the dynamic solids volume fraction. - The results of gas-solids mass transfer measurements for circulating fluidized bed unit were investigated.	1994	[67]
21	Intalox saddles, raschig ring	FCC	- The pressure gradient and powder hold-up in the packing were measured in a rectangular fluidized bed. - A mathematical analysis for the prediction of pressure drop, which was caused by the powder hold-up and the friction between gas and packing and between powders and packing, were proposed.	1995	[23]

Table 1(continue): Summary of investigations on packed-fluidized bed concept.

No.	Packing	Bed material	Results	Year	Ref.
22	-	-	- A review of fluid dynamics studies of counter-current gas-solid contactors were presented. - The experimental and mathematical models in research findings about the basic fluid dynamics parameters: flowing solids holdup, pressure drop and flow pattern were gathered.	2007	[68]
23	Raschig rings, ceramic beads, crushed stone and glass beads	Sand, propant, alumina and glass	- Static holdup was investigated experimentally and theoretically in packed-fluidized bed contactors. - The experimental results showed a significant influence of the geometry of the packing elements on static holdup. The physical properties of the flowing solids also influenced static holdup. A moderate influence of solids flux and a minor influence of gas velocity were observed. - An empirical correlation for the prediction of static holdup was developed from theoretical and numerical analyses.	2009	[69]
24	Coarse spheres	Geldart B particles	- The dependence of bed voidage on fluidization velocity and particle properties was investigated. - Their analysis leaded to new relationships for calculating the parameters of the Richardson-Zaki correlation. Thus, providing a quantitative interpretation of the expansion process of packed-fluidized beds.	2011	[46]
25	Spherical lead shots and spherical glass bead	Glass ballotini	- They investigated the criteria for obtaining a homogeneous fluidization in packed-fluidized bed. The criteria regarded: the choice of the size of particles constituting the packed bed and the packing height necessary to accommodate the desired level of voidage; the minimum aspect ratio of the confined bed that guarantees the minimum fluidization velocity to be independent of the bed mass; and the packed bed height required to operate the particle system over a broad field of homogeneous expansion. - They modified the Richardson-zaki equation to model the homogeneous regime.	2013	[70]
26	-	-	- A counter-current fluidized bed reactor for the dehydrogenation of olefins was patented. - The process utilized a reactor that included a slower flow of catalyst through the reactor, with a counter current flow of gas (process stream) through the catalyst bed.	2015	[71]
27	Active carbon, glass balls (Ballotini), activated alumina, silica gel	Glass balls	- Confined fluidization of fines in fixed bed of coarse particles was investigated. - Relations allowing calculation of the Richardson-Zaki-type equation coefficients, including description of inter-particle void and gas pressure drop in such systems were determined.	2016	[53]
28	Coarse spheres	Geldart B particles	- They presented a model to predict the minimum fluidization velocity of beds of Geldart's group B particles confined in a packed-bed of coarse spheres.	2016	[72]
29	Spherical packing	Zeolites	- CO_2 adsorption by a fluidized bed of pellets of 13X zeolite was investigated. - The experiments compared the performance of a confined and that of a conventional fluidized bed at ambient temperature and pressure. - They demonstrated that confined fluidization improved the efficiency of the adsorption process compared to the conventional technique.	2017	[54]
30	Lithium titanate (Li_2TiO_3) pebble	Li_2TiO_3	- Results showed that the effective thermal conductivity of packed fluidized bed increased close to the value of thermal conductivity of pure Li_2TiO_3 at an optimum fluidization velocity corresponding to 2–3 times minimum fluidization velocity depending on fluidized particle, size, its volume fraction and wall temperature.	2017	[43]

Table 1(continue): Summary of investigations on packed-fluidized bed concept.

No.	Packing	Bed material	Results	Year	Ref.
31	Coarse glass sphere	Zeolite	- They performed CO_2 adsorption across a packed-fluidized bed compared with traditional fixed bed adsorption. - The packed fluidized system allowed operation across a wide-range of gas velocities without a substantial increase in pressure drop. -Packed-fluidized bed prevented the formation of bubbles in favor of enhancing the bed expansion ability.	2019	[55]
32	Spherical packings (ECA, ASB)	Ilmenite	- Chemical-looping combustion with ilmenite as oxygen carrier was studied in a packed-fluidized bed with spherical packings. Syngas and CO was used as fuel at 915 °C. Results showed that in packed-fluidized bed, the effective reaction rate constant increased by up to a factor of 2 for a given bed mass compared to conventional fluidized beds. - Up to 4 times less oxygen carrier bed mass was needed to achieve the same gas conversion in a packed-fluidized bed, at a lower total pressure drop.	2019	[12]
33	Spherical packings (ECA, ASB)	Silica gel and olivine sand	- Packed-fluidized bed concept was applied to investigate the effect of packings on gas-solid mas-transfer. For mass transfer experiments the fluidizing air was humidified and the water adsorption rate onto silica gel particles acting as fluidizing solids was measured. - It was found that mass transfer increased by a factor of 1.9–3.8 with packing solids as compared to a non-packed reference. - Maximum vertical cross-flow was found to be significantly higher with low density packing (ECA) that fluidized, than with stationary high-density packing (ASB).	2019	[40]

Through these investigations, it is clear that substantial advantages can be realized by use of packed-fluidized beds. Possible advantages that have been identified includes avoiding agglomeration for some special applications, improving the heat transfer properties, better temperature control, reducing the stagnant regions and improving fluidization, increased overall conversions and efficiencies and elimination of bubble growth.

Packed-fluidized beds could be of high interest for CLC. The reason is not difficult to grasp. In CLC, it is absolutely critical to achieve high mass-transfer rate between gas and oxygen carrier throughout the whole bed. This is because gaseous fuel species must get in physical contact with the solid oxygen carrier, in order to be converted to products. In contrast to normal fluidized bed combustion, in CLC, it cannot be expected that residual combustible components can be converted in the freeboard. Aronsson et al. investigated the effect of using spherical aluminum silicate balls (ASB) and expanded clay aggregate (ECA) as packings during CLC batch experiments [12]. They observed that these packings can improve fuel conversion. However, they could also result in increased pressure drop inside the bed and particle segregation phenomena [12], [40]. Thus, there is still a lack of investigation for other types of relevant packings like the effect of a more evolved RMSR and Hiflow packings, and the theory behind the enhanced mass transfer.

3 Method

3.1 Experimental

Throughout the work reported in this licentiate thesis (**Papers I–III**), two different experimental reactors have been used, both of which utilize the same furnace and most other infrastructure. More detailed information about the common dimensions of the two laboratory-scale bubbling fluidized bed reactors are summarised in Table 2.

Table 2: Summary of the two laboratory experimental setups used for experiments.

Specification	**Papers I- III**
Reactors:	
I.D. (mm)	78
Height (mm)	1270
Distribution plates:	
Type	Circular hole plate
Thickness (mm)	5
Number of holes (-)	61
Hole I.D. (mm)	0.6

In **Paper I**, the effect of packed-fluidized bed on heat transfer at elevated temperature levels was studied. Figure 6 provides a schematic illustration of the reactor used in **Paper I**.

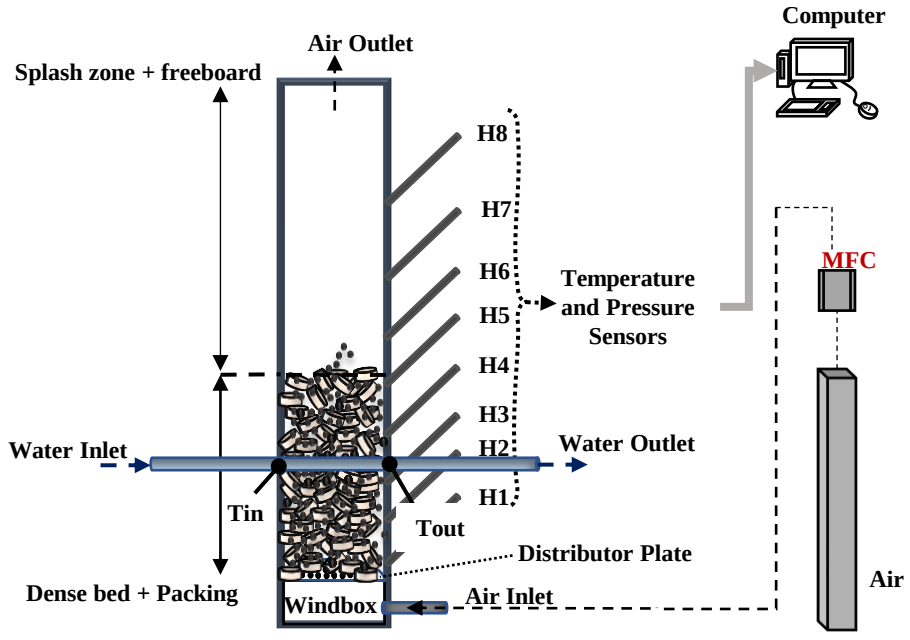

Figure 6: Schematic illustration of reactor for heat transfer experiments, used in Paper I.

For **Paper I**, a 253 MA steel reactor was equipped with a single horizontal tube made of Inconel 600 alloy. The inner diameter of the horizontal tube was 4 mm, and the wall thickness was 1 mm. The horizontal tube was positioned 75 mm above the gas distributor plate (Table 3). In all experiments, the horizontal tube was in the dense bed; and it was covered with the packing and bed material. Water flowed through the horizontal tube from a tap. The flow rate was regulated with a valve. During all experiments, the water flow rate through the pipe used for measuring heat transfer coefficient was kept constant at 20 ml/s. Heat transfer coefficient was calculated from the temperature rise measured from the inlet to the outlet of the horizontal pipe.

Table 3: Vertical position of measurement points relative to the distributor plate.

	Paper I		**Paper II**		**Paper III**	
Position	**Height (mm)**	**Measured data**	**Height (mm)**	**Measured data**	**Height (mm)**	**Measured data**
Windbox	-	Temperature & Pressure	-	Temperature & Pressure	-	Temperature & Pressure
1	30	Temperature	36.5	Temperature & Pressure	36.5	Temperature & Pressure
2	47	Pressure	88.8	Temperature & Pressure	88.8	Temperature & Pressure
3	65	Temperature	136.5	Temperature & Pressure	136.5	Temperature & Pressure
Water tube	75	Temperature	-	-	-	-
4	105	Temperature	156.5	Temperature & Pressure	156.5	Temperature & Pressure
5	130	Pressure	316.5	Temperature & Pressure	316.5	Temperature & Pressure
6	150	Temperature	476.5	Temperature, Pressure & gas concentration	476.5	Temperature & Pressure
7	310	Pressure	636.5	Temperature, Pressure & gas concentration	636.5	Temperature & Pressure
8	605	Pressure	796.5	Temperature & Pressure	796.5	Temperature, Pressure & gas concentration

In **Papers II-III**, the impact of packed-fluidized bed on fuel conversion rate in CLC was investigated. A schematic description of the batch CLC reactor used in **Papers II-III** is depicted in Figure 7. For this study, eight horizontal measurement tubes were added to the front side of a 235 MA steel reactor, to allow for connecting gas sampling tubes (Table 3). Normally, only one of the front tubes was used at each time for gas sampling. Since the fuel conversion rate is a key factor that needs to be verified at the outlet of the bed, the gas samples were taken from sampling points 6, 7 and 8 (depending on the bed height). The measurement points were chosen to assure that the outlet concentration of gases leaving the bed was analyzed in the freeboard, rather than inside the bed or the splash zone. The sample of gas was taken to a gas analyzer SICK GMS810. Sampling was done via a PTFE tube heated to 190 °C, to ensure that condensation prior to the gas conditioning system did not occur. The SICK GMS810 gas analyzer measured the composition of gas in volume percent (vol%) for relevant gas components, including CO_2, CO, H_2, CH_4 and O_2.

The heat needed to reach the desired reactor temperature was provided by an electric furnace enclosing the reactor. Since the windbox was located inside the furnace, the fluidization gas was pre-heated essentially to the bed temperature, already before entering the reactor. The hot gas exiting the reactor was collected by a ventilation hood located above the reactor exit.

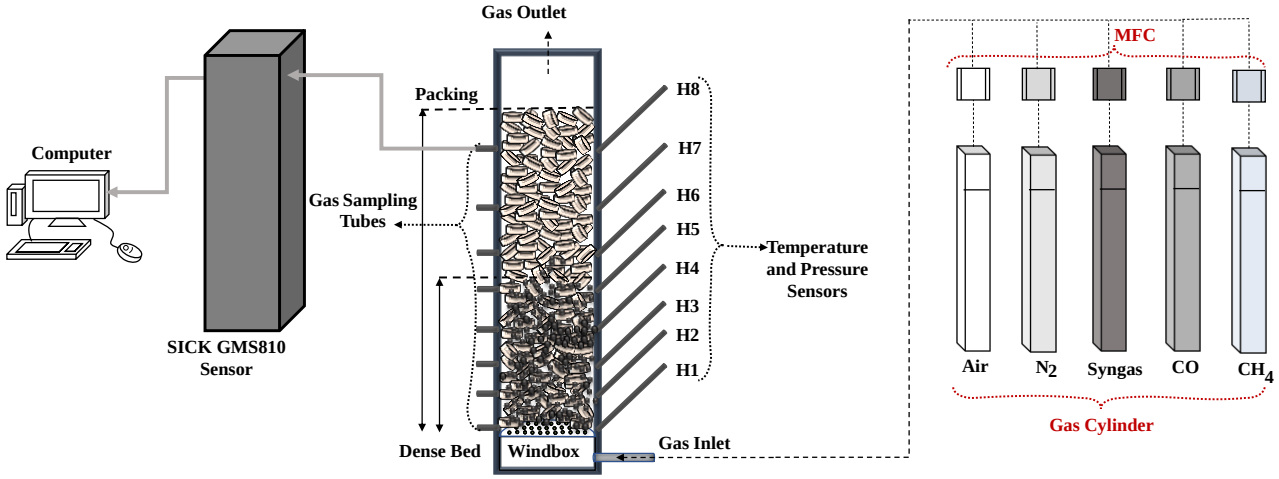

Figure 7: Schematic illustration of reactor for batch CLC reactions in Papers II-III.

3.2 Bed material and packings

In **Paper I** the bed material used in experiments was silica sand supplied by Sibelco Nordic AB. It was sieved to the size range of 90-400 µm. The mean particle diameter was calculated to 240 µm. Bulk density of the bed material used in **Paper I** was 1594 kg/m^3. In **Papers II–III** ilmenite concentrate was chosen as the bed particles and oxygen carrier. The reason is that this is one of the most studied and possibly the most reliably performing oxygen carrier for CLC. Ilmenite concentrate is the crushed and beneficiated form of the mineral ilmenite, which is an ore mined for production of TiO_2. Ilmenite ore consists mainly of iron and titanium oxides ($FeTiO_3$, Fe_2TiO_5, Fe_2O_3, TiO_2, Fe_3O_4). Ilmenite concentrate is ore that has been ground and physically beneficiated to increase the content of iron and titanium oxides. In **Papers II–III**, ilmenite particles that previously had been utilized as bed material in a CLC pilot reactor was used. The batch of particles was originally generated in the campaign by Moldenhauer et al. [73], and have previously also been used in other experimental studies [12], [74]. The reason for using this batch of material is to ensure that the particles had reached steady-state conditions. Fresh ilmenite used for CLC experiences swelling and activation during the first few dozens of redox cycles. The measured bulk density of the particles used was 1637 kg/m^3. The ilmenite particles were sieved to the size range 90-250 µm. The average diameter of particles was 179 µm.

Packings used in **Papers I–III** were 25 mm stainless steel thread saddle (RMSR), 25 mm stainless steel pall ring (Hiflow), 6 mm ceramic Raschig ring (RR6), 10 mm ceramic Raschig ring (RR10), and 12.7 mm aluminum silicate balls (ASB). Table 4 lists the packings used in each paper with the information on their void factor, bulk density, and packing height.

Table 4: Description and characteristics of packings used in Papers I-III.

Packing	Void factor (-)	Bulk density (kg/m^3)	Packing height (mm)		
			Paper I	Paper II	Paper III
RMSR	0.96	204	130	1000	1000
Hiflow	0.95	280	130	-	1000
RR6	0.50	1110	130	-	-
RR10	0.58	890	130	-	-
ASB	0.43	1390	130	1000	-

3.3 Gases

For the experiments in **Paper I**, air was used as the fluidizing gas. Superficial gas velocity was varied in the range of 0.04-0.411 m/s. In **Paper II**, investigated fuel gases were carbon monoxide (CO) at 840 °C and methane (CH_4) at 940 °C. The reason for using these fuel gases for this work is the well-established difference in the reaction rate in CLC for these two gases, when using ilmenite as oxygen carrier. Thus, since the aim of the study was to examine the impact of packing materials, rather than the impact of temperature on the reactivity of ilmenite with fuel gases, the temperature levels were chosen so that high but not complete fuel conversion could be expected. By doing so, any improvement when using packings could be seen clearly. In **Paper III**, fuel gases were syngas (50/50% H2/CO) and CO at 840 °C. Syngas is a representative fuel for practical applications. CO was used since it simplifies data evaluation and could make it easier to draw firm conclusions and support modelling. In **Papers II-III**, nitrogen (N_2) was used as inert gas. Air was used as the oxidizing gas. The total gas flow rate of 21 L_n/min was used in the oxidation and reduction steps for **Papers II-III**.

3.4 Data Evaluation

3.4.1 Bed-to-tube heat transfer coefficient

In **Paper I**, bed-to-tube heat transfer coefficient, h_o, was calculated applying the overall heat transfer coefficient formula through a tube. The equations used to calculate h_o in **Paper I** are summarized in Table 5 [75–77].

Table 5: The equations used to calculate h_o in Paper I.

Bed-to-tube heat transfer coefficient	$h_o = \frac{1}{\frac{1}{U_o} - \frac{d_o \ln(d_o/d_i)}{2k_{wall}} - \frac{d_o}{d_i h_i}}$	(1)
Overall heat transfer coefficient ($W.m^{-2}K^{-1}$)	$U_o = \frac{Q}{A_o \Delta T_{LM}}$	(2)
Logarithmic mean temperature (K)	$\Delta T_{LM} = \frac{\Delta T_{in} - \Delta T_{out}}{\ln(\Delta T_{in}/\Delta T_{out})}$	(3)
Inlet side temperature difference (K)	$\Delta T_{in} = T_{bed} - T_{water,inlet}$	(4)
Outlet side temperature difference (K)	$\Delta T_{out} = T_{bed} - T_{water,outlet}$	(5)
Heat transfer rate between bed and water flow	$Q = \rho_{water} \dot{V} c_{p,water} (T_{water,outlet} - T_{water,inlet})$	(6)
Heat transfer coefficient from tube wall to water ($W.m^{-2}K^{-1}$)	$h_i = 0.023 \frac{k_{water}}{d_i} Re^{0.8} Pr^{0.4}$	(7)
	$h_i = \frac{k_{water}}{d_i} j_h Re Pr^{0.33}$	(8)
	$h_i = \frac{4200(1.35 + 0.02 T_{water,avg}) u_{water}^{0.8}}{d_i^{0.2}}$	(9)
Temperature of inside of tube wall (K)	$T_{wall,in} = \frac{Q}{h_i A_i} + T_{water,avg}$	(10)
Temperature of outside of tube wall (K)	$T_{wall,out} = Q \frac{d_o \ln(d_o/d_i)}{2k_{wall} \times A_o} + T_{wall,in}$	(11)

3.4.2 Vertical segregation in packed-fluidized-beds

A bed of stationary packings and fluidizing particulate materials will divide into two distinct regions at high superficial gas velocities [40]. The bottom region is made up of packings and fluidized particles. Also, a dense phase of segregated fluidizing solids will accumulate on its top. In **Paper I**, by placing a pressure sensor at the height where the packed region ends in the

resting state of reactor (13 cm above distributer plate), the pressure drop induced due to segregation above the packing can be measured accurately. As described in **Paper I**, the relation between the void fraction and the fluidizing particle mass inside the packing is given by equation (12).

$$\varepsilon_{p,packing} = (\frac{1-\varepsilon_p}{m_{p,tot}})m_{p,top} + \varepsilon_p \quad (12)$$

where, ε_p is the void fraction of particles at rest.

3.4.3 Fuel conversion

For the gas fuels used in **Paper II** (CO and CH_4) and **Paper III** (CO and syngas, 50/50% H_2/CO) conversion equations are listed in Table 6.

Table 6: The equations used to calculate fuel conversion in Papers II- III.

Reactions:		
CO and oxygen carrier	$CO + M\_O \rightarrow CO_2 + M$	(13)
CH_4 and oxygen carrier	$CH_4 + 4\,M\_O \rightarrow CO_2 + 2H_2O + 4\,M$	(14)
Syngas and oxygen carrier	$CO + H_2 + 2M\_O \rightarrow CO_2 + H_2O + 2M$	(15)
Fuel conversion:		
Conversion of CO (-)	$\gamma_{CO} = \frac{n^{\cdot}_{CO_2,out}}{n^{\cdot}_{CO,out} + n^{\cdot}_{CO_2,out}}$	(16)
Conversion of CH_4 (-)	$\gamma_{CH_4} = \frac{n^{\cdot}_{CO_2,out}}{n^{\cdot}_{CH_4,out} + n^{\cdot}_{CO_2,out} + n^{\cdot}_{CO,out}}$	(17)
Conversion of syngas (-)	$\gamma_{syngas} = \frac{n^{\cdot}_{CO_2,out} + n^{\cdot}_{H_2,in} - n^{\cdot}_{H_2,out}}{n^{\cdot}_{CO,out} + n^{\cdot}_{CO_2,out} + n^{\cdot}_{H_2,in}}$	(18)
Conversion of H_2 (-)	$\gamma_{H_2} = \frac{n^{\cdot}_{H_2,in} - n^{\cdot}_{H_2,out}}{n^{\cdot}_{H_2,in}}$	(19)
Conversion of oxygen carrier:		
Oxygen carrier conversion (-)	$X = 1 - \frac{m}{m_{ox}}$	(20)
Momentary conversion for CO (-)	$X_i = X_{i-1} + \int_{t-1}^{t} \frac{n^{\cdot}M_O}{m_{ox}}(y_{CO_2})dt$	(21)
Momentary conversion for CH_4 (-)	$X_i = X_{i-1} + \int_{t-1}^{t} \frac{n^{\cdot}M_O}{m_{ox}}(4y_{CO_2} + 3y_{CO} - y_{H_2})dt$	(22)
Momentary conversion for syngas (-)	$X_i = X_{i-1} + \int_{t-1}^{t} \frac{n^{\cdot}M_O}{m_{ox}}(2y_{CO_2} + y_{CO} - y_{H_2})dt$	(23)

3.4.4 Reaction contact factor and gas interchange coefficient

In **Paper III**, the effective reaction contact factor, which is the multiplication of contact efficiency and reaction rate constant for the combustion experiments, is estimated as k_f ($Nm^3kg^{-1}s^{-1}$).

Further, packings will affect the reaction rate through changing the mass transfer rate between bubble phase and emulsion phase. This is believed to be one of the principal bottle necks for converting fuel to CO_2 with CLC (**Papers II-III**). In other words, packings will affect the mass transfer rate by changing the surface area between bubbles and emulsion, through affecting the bubble size. Thus, in **Paper III**, a model for calculating average bubble size, d_b (m), and then, the overall interchange coefficient between bubble phase and emulsion phase, K_{be} (s^{-1}) was

introduced. For this purpose, the two-phase theory model was applied. The details will be described in Table 7.

Table 7: Reaction contact factor and gas interchange coefficient presented in Paper III.

Effective reaction contact factor ($Nm^3kg^{-1}s^{-1}$)	$k_f = \eta \times k_r = \frac{\alpha F_0}{m}$	(24)
Overall gas exchange coefficient between bubble and emulsion (s^{-1})	$K_{be} = \frac{1}{\frac{1}{K_{bc}} + \frac{1}{K_{ce}}}$	(25)
Gas exchange coefficient between bubble and cloud (s^{-1})	$K_{bc} = 4.5\left(\frac{u_{mf}}{d_b}\right) + 5.85(\frac{D^{1/2}g^{1/4}}{d_b^{5/4}})$	(26)
Gas exchange coefficient between cloud and emulsion (s^{-1})	$K_{ce} = 6.77\left(\frac{D\varepsilon_{mf}u_{br}}{d_b^3}\right)^{1/2}$	(27)
Minimum fluidization velocity (m/s)	$\frac{d_p u_{mf}\rho_g}{\mu} = \left[(28.7)^2 + 0.0494\left(\frac{d_p^3\rho_g(\rho_s-\rho_g)g}{\mu^2}\right)\right]^{1/2} - 28.7$	(28)
Void fraction in bed at minimum fluidization (-)	$\frac{1.75}{\varepsilon_{mf}^3\emptyset_s}\left(\frac{\rho_P u_{mf} d_P}{\mu_g}\right)^2 + \frac{150(1-\varepsilon_{mf})}{\varepsilon_{mf}^3\emptyset_s^2}\left(\frac{\rho_P u_{mf} d_P}{\mu_g}\right) = Ar$	(29)
Void fraction in the fluidized bed (-)	$\varepsilon_f = 1.5\left(\frac{\sigma}{0.438\rho_P g L}\right)^{0.8896} Ar^{-0.0211}(\frac{L}{D_c})^{-0.388}$	(30)
Bubble diameter (m)	$d_b = \frac{1}{(0.711)^2 g}\left[u_{mf} + (u_o - u_{mf})\frac{1-\varepsilon_{mf}}{\varepsilon_f - \varepsilon_{mf}}\right]^2$	(31)

4 Results

4.1 Effect of packing on bed-to-tube heat transfer coefficient and vertical segregation

The effect of temperature and superficial gas velocity on bed-to-tube heat transfer coefficient in packed-fluidized beds are investigated in **Paper I**. For the effect of temperature on heat transfer coefficient, results were illustrated at the fixed superficial gas velocity of 0.2 m/s. Results showed that at this superficial gas velocity, heat transfer coefficient varied significantly (671-1298 W/m^{2}K) in the temperature range of 400-900 °C (Figure 8).

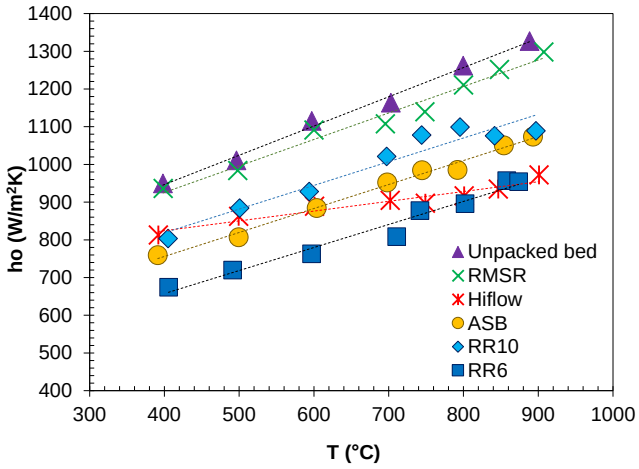

Figure 8: Effect of bed temperature on bed-to-tube heat transfer coefficient in packed-fluidized beds: superficial gas velocity 0.2 m/s, water flow rate 20 ml/s, stagnant bed and packing height 13 cm, source: ***Paper I****.*

At superficial gas velocity of 0.2 m/s, the bed with no packings showed a higher heat transfer coefficient at all temperatures compared to packed-fluidized beds. However, it can be observed in **Paper I** that RMSR performed essentially equal as the bed with no packings. RR10 displayed the second highest heat transfer coefficients with increasing bed temperature with almost the same trend as ASB. It was showed in **Paper I** that for RR6 heat transfer coefficient decreased compared to RR10. The reason is probably that smaller packings restrict particle movements more and thus decrease heat transfer inside the bed. Since by decreasing the size of RRs from 10 mm to 6 mm, bed restriction and channeling could be expected to intensify. Another finding in **Paper I** was that despite the similar attributes of Hiflow packings to RMSR with respect to nominal size and void factor, the heat transfer when using Hiflow packing was significantly less good than for RMSR packings. This result was discussed in more details in **Paper I**.

The second target of **Paper I** was to evaluate the effect of superficial gas velocity on bed-to-tube heat transfer coefficient. For this purpose, the temperature was kept constant at 800 °C. As described in **Paper I**, at high superficial gas velocities, packed-fluidized bed with RMSR

packings shows higher heat transfer coefficient (1243 W/m^{2}K) compared to other cases including to the bed without packing, which displayed a maximum heat transfer coefficient of 1124 W/m^{2}K (Figure 9).

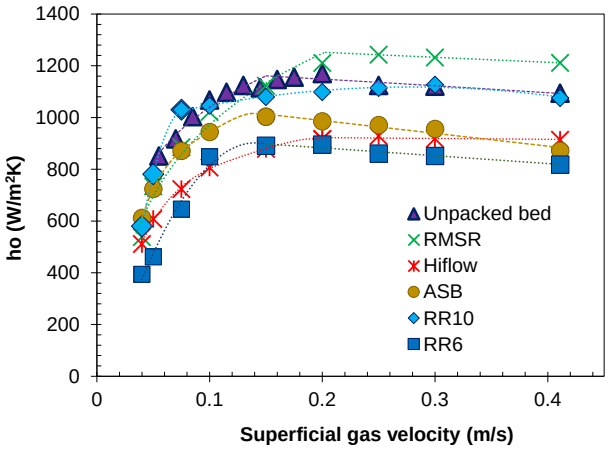

Figure 9: Effect of superficial gas velocity on bed-to-tube heat transfer coefficient in packed-fluidized beds: temperature 800 ℃, water flow rate 20 ml/s, stagnant bed height 13 cm, source: ***Paper I****.*

The reason for improvements with packings was attributed to their ability to break large bubbles into smaller ones which was further investigated in **Papers II-III**. To facilitate understanding, the behavior of a bed with no packing and increasing gas velocity can be considered. The particulate bed can in this case be divided in two different phases, the emulsion phase and the bubble phase. By increasing gas velocity at a fixed temperature, initially, formation of small bubbles will help increasing the interaction of bed particles with each other and the surface of the water tube. Thus, it will increase heat transfer between bed material and tube. However, increasing gas velocity to higher values will increase the number of bubbles. Eventually, bubbles coalescence will occur and result in formation of bigger bubbles. Since heat transfer is a function mainly of particles coming in direct contact with the tube, this will reduce the heat transfer coefficient. A packing with high void factor such as RMSR, that does not greatly hinder particle movement but breaks down big bubbles to smaller ones, could therefore conceivably improve heat transfer coefficient to a submerged tube, as have been observed in Figure 9.

Another aim of **Paper I** was to evaluate the effect of packings on vertical segregation of fluidizing solids. These results are of importance since high segregation will result in less bed material to retain in the packed zone. Therefore, the heat transfer will reduce subsequently in this part of the bed. **Paper I** showed that Hiflow and RMSR packings were much better to retain bed material in the packed zone up to 13 cm reactor height than the other packings, which suffered from larger tendencies towards vertical segregation at high velocities. For almost all packings (except Hiflow) there was a clear correlation between the amount of bed material retained in the packed zone and heat transfer coefficient (Figure 9, Figure 10).

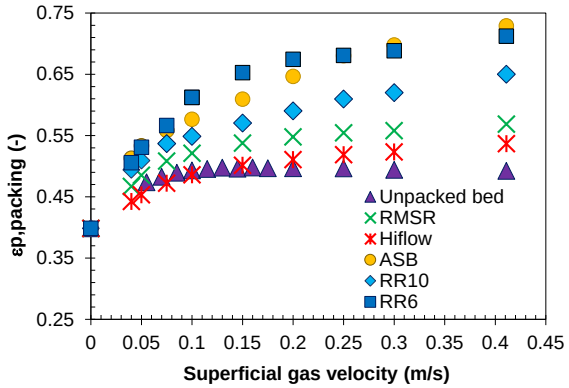

Figure 10: Voidage of fluidizing solids as function of superficial gas velocity for different packings: pressure probe at 13 cm above distributer plate, temperature 800 ℃, water flow rate 20 ml/s, stagnant bed packing height 13 cm, source: ***Paper I****.*

4.2 Effect of packing on fuel conversion in CLC

Based on the findings of **Paper I** on packing's behaviour and their characteristics, different pairs of packings were selected for further investigations in **Papers II-III**. In **Paper II**, RMSR with high void factor (0.96) was compared to ASB with low void factor (0.43). In **Paper III**, the two high void factor packings RMSR (0.96) and Hiflow (0.95) were studied. The average fuel conversion in **Papers II-III** was depicted as function of bed height for the studied packings (Figure 11 and Figure 12).

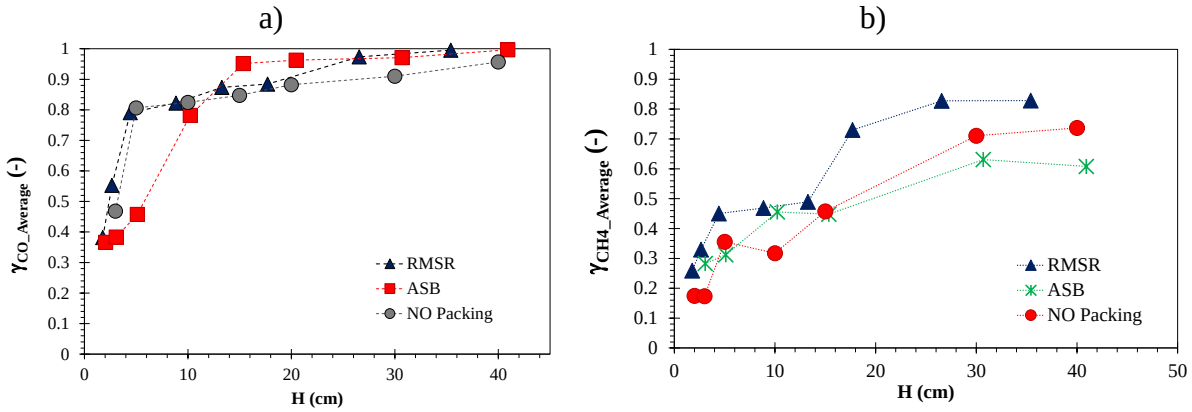

Figure 11: Average fuel conversion as function of bed height, a) CO at 840 ℃, b) CH_4 at 940 ℃, source: ***Paper II****.*

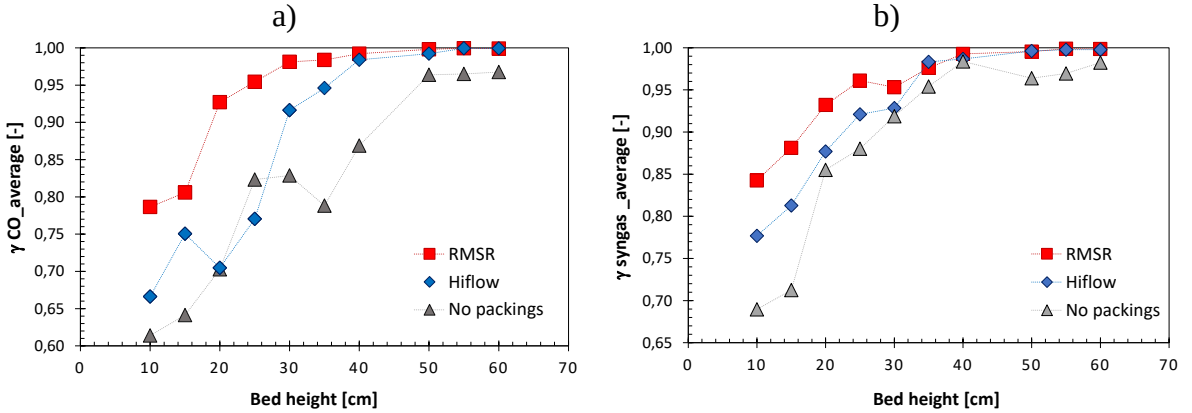

Figure 12: Average fuel conversion as function of bed height, a) CO at 840 ℃, b) syngas at 840 ℃, source: ***Paper III****.*

General finding in **Papers II-III** was that RMSR showed the most significant improvements. The main reason for better fuel conversion with RMSR packings was attributed to the ability of this packing to increase the mass transfer rate, presumably by breaking down bubbles. At the same time, RMSR packing still allows for similar bed mass for a given volume as an unpacked bed. This is in stark contrast to the ASB packings. Also, the RMSR packings packed more easily in the experimental reactor, as compared to the bulkier Hiflow packings. In **Paper II**, it was shown that with bed depths lower than approximately 15 cm the effect of adding packings is not clear in fuel conversion (Figure 11a). The likely reason is that the packing materials used has the nominal dimensions of 12.7 mm and 25 mm. For low bed heights this means that the packing depth is only a few stacked layers of packing, which may be insufficient to achieve an even flow profile. Also bubble size could be expected to be small with low bed height, leaving limited space for improvement.

In the next step, in **Papers II-III**, average fuel conversion was investigated as a function of pressure drop. **Papers II-III** showed that for all the studied packings, there is a significant improvement in fuel conversion for given pressure drop, for the cases which corresponds to deeper bed heights than 5 cm. **Papers II-III** showed that the pressure drop for a given conversion of fuels was lower in the packed beds compared to the other alternative without packings (Figure 13 and Figure 14).

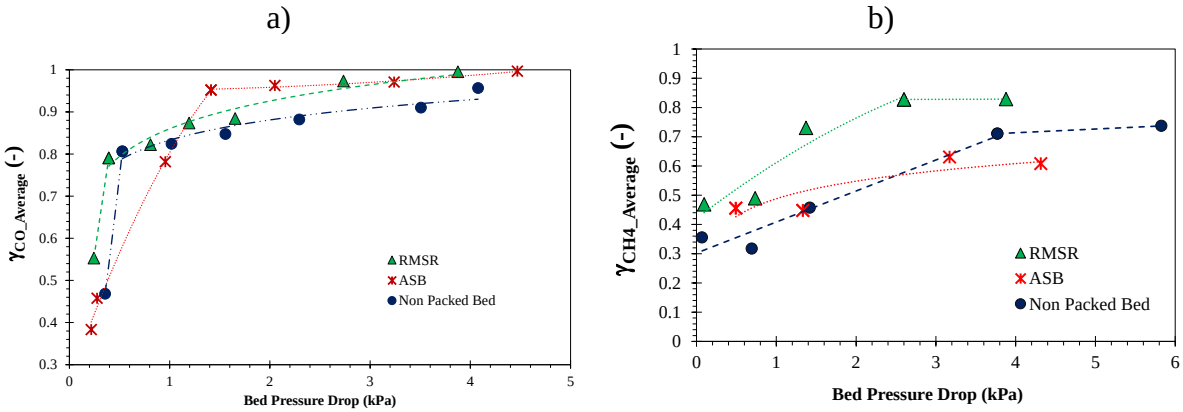

Figure 13: Average fuel conversion as function of bed pressure drop, a) CO at 840 ℃, b) CH4 at 940 ℃, source: ***Paper II****.*

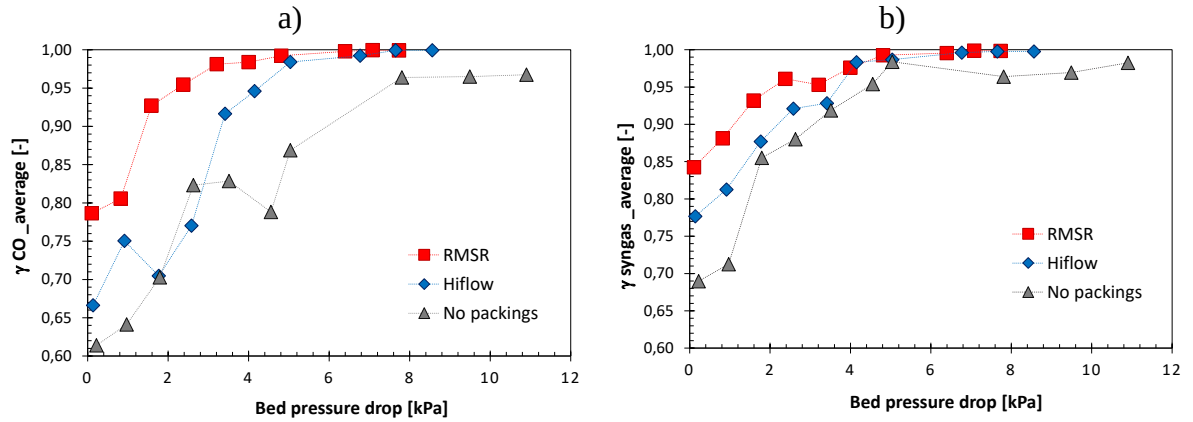

Figure 14: Average fuel conversion as function of bed pressure drop, a) CO at 840 ℃, b) syngas at 840 ℃, source: ***Paper III****.*

4.3 Effect of packings on reaction contact factor and gas interchange coefficient

In the last section of **Paper III**, the increased fuel conversion was studied in more depth, and an attempt was made to characterize the mass transfer based on bubble size as well as gas-solid contact efficiency. As described in chapter 3 section 3.4.4, the behaviour with respect to bubbles was explored through pressure signal data (**Paper III**). This could result in further insights on the effect of packings in the bed. Thus, **Paper III** took its initial step in investigating bubble size. The average bubble diameter was calculated with equation (31) in the previous section. The results are shown in Figure 15.

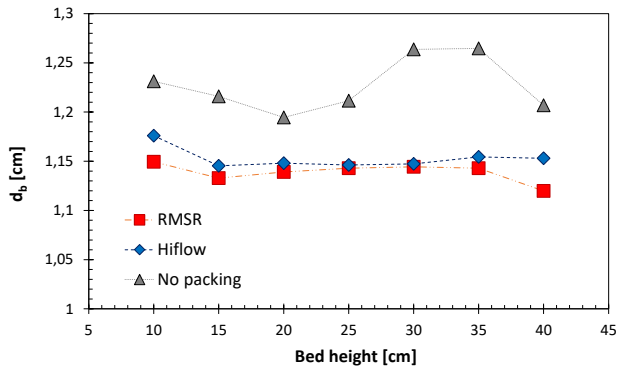

Figure 15: The changes of bubble diameter as function of bed height, as estimated by equation (31): Pressure data gathered and analyzed at MP1 using a measurement frequency of 1 Hz, source: ***Paper III****.*

Figure 15 shows the changes of bubble diameter as calculated from the standard deviation of pressure signal data gathered at MP1, located at 3.65 cm above the distributor plate. This measurement point was chosen to assure that for all the bed heights, pressure sensor is inside the bed. Thus, the signals will be related to bubble formation, coalescence, eruption etc. in the packed-fluidized bed and not in the splash zone. The results can be assumed to represent an estimation of an average value (**Paper III**). As discussed in **Paper III**, bubble diameter in packed beds containing high void packings of RMSR and Hiflow are very close to each other and around 8 % less than beds without packings. Thus, the surface area where gas inter or exit the bubble decrease by 17% and the gas volume in each bubble decreases 25% (Figure 15). It is worth pointing out that bubbles would be expected to grow larger in deeper beds, so for real-world applications of CLC bubble growth could be a very significant issue.

In the final step in **Paper III**, the reaction contact factor, k_f ($Nm^3kg^{-1}s^{-1}$), and gas interchange coefficient, K_{be} (s^{-1}), were calculated with equations (24) and (25), respectively. Then, they were illustrated as a function of bed height. As it is expected that the intrinsic rate constant k_r, in eq. (24) would be constant for a certain material, k_f can be seen as an effective contact factor between bed material and gas, and hence a gauge of improved mass-transfer. **Paper III** indicated that applying RMSR and Hiflow packings will improve both K_{be} and k_f in the system, compared to a bed with no packings. This improvement is more significant for RMSR packing. As mentioned in **Papers I-III**, the void factor of both packings is similar to each other (more than 95 %). This difference in performance between the packings could be due to geometry. For the RMSR packing, more uniform beds with smaller bubbles may be formed and consequently the improvements are more pronounced than for Hiflow packings. Also, the Hiflow packings are bulkier and this pack less flawlessly in the reactor. Thus, they can be expected to suffer from more significant wall effects. This conclusion was in accordance with

Paper I, where the heat transfer in the packed- fluidized beds for these packings was investigated.

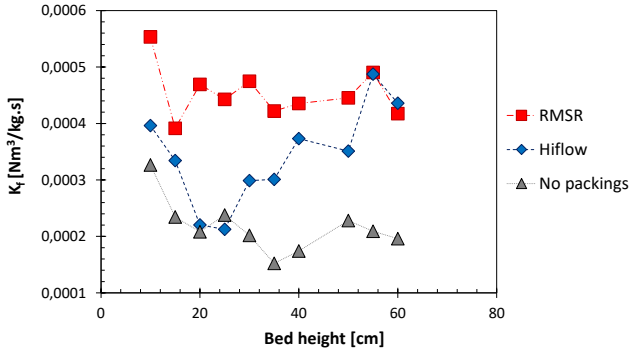

Figure 16: k_f as calculated by equation (24) as a function of bed height: Pressure data gathered and analyzed at MP1, source: ***Paper III****.*

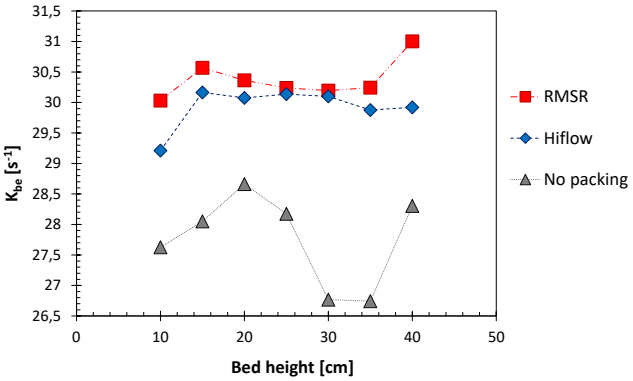

Figure 17: K_{be} as calculated by equation (25) as a function of bed height: Pressure data gathered and analyzed at MP1, source: ***Paper III****.*

5 Discussion, conclusions, and future work

5.1 Discussion

The use of packed-fluidized beds has been investigated in this work, through **Papers I-III**. The experiments have been performed at elevated temperature, and the general idea has been to apply packings to improve performance of CLC. In general, packings studied in this thesis can be divided in two main categories, namely high void factor packings (RMSR and Hiflow) and low void factor packings (ASB, RR6 and RR10). High void packings should be easily applicable to circulating fluidized bed systems, as they are not expected to hinder e.g. solids flux or reactor inventory to significant extent. Low void packings would require a more significant engineering effort to be feasible for CLC but represents a different range of possibilities.

Paper I showed that packings with low void factor will increase the pressure drop per mass of fluidized particles in the bed. This will cause in much more pronounced vertical segregation compared to a bed without packings (**Paper I**). Thus, with respect to heat transfer to a pipe inserted inside the bed (**Paper I**), packings of this type will cover parts of the outer surface of the horizontal tube and decrease the efficient surface area for direct particle to tube heat transfer. Packings with high void factor should not have the same impact on heat transfer. In fact, it is shown that RMSR can be applied with little negative or even positive effect. The results for Hiflow packings are less good. The reason for this is not totally clear and is discussed in detail in **Paper I**. In fact, the impact on heat transfer by Hiflow packings may be the single most uncertain result in the studies included in this thesis.

However, on the other hand, as discussed in **Paper II**, all types of packings will physically constrain bubble size. Thus, packed- fluidized beds (regardless of packing voidage) can improve the average conversion of fuel gas to values higher than non-packed beds, by preventing bubble growth and by breaking down bigger bubbles into smaller ones. However, it is important to point out that the gas-solid mass transfer is only one factor influencing fuel conversion in CLC. Reaction kinetics between the fuel and oxygen carrier is another very important factor, which can differ greatly for different combinations and process parameters (temperature, bed material, fuel etc.). Packings will affect the fuel conversion only if mass transfer is a significant bottleneck, which for current experiments seems to be the case for deep beds (heights greater than 15 cm as discussed in **Paper II**). For the two high void packings (RMSR and Hiflow), **Paper III** showed that the mass transfer of gas between phases can be enhanced considerably using both packings. This can have implications for many fluidized bed technologies, such as for example chemical-looping combustion (CLC). As illustrated in **Paper III**, beyond 40 cm bed height with RMSR or Hiflow packings, the fuel conversion is approaching 100%. At lower bed heights, effects from large bubbles or slugging are unlikely to be a factor as these do not have sufficient time for bubbles to coalesce. It can be concluded

that fuel conversion is increased in packed beds compared to beds without packing. When the results from experiments using RMSR, Hiflow or no packings are compared (**Paper III**), the RMSR has the highest overall fuel conversion regardless of bed height or fuel type. As shown in Table 4, both RMSR and Hiflow packings have a similar void factor (more than 95 %), thus the difference between RMSR and Hiflow packings should be due to their geometries. Experimental results observed in **Paper III** point to RMSR having a more suitable geometry for bubble eliminations in general. RMSR has an asymmetric shape that possibly creates a tighter lattice structure, compared to the more symmetrically shaped Hiflow packings. A tighter lattice structure might be preferable in terms of bubble inhibition that leads to more effective bubbling fluidization. Alternatively, it can be hypothesized that the bulkier Hiflow packings will distribute less well in the relatively small reactor vessel used here. This may result in unfavorable flow phenomena, such as bypass flow near the reactor wall. However, this cannot be easily observed in steel reactors.

5.2 Conclusions

In this work, the effect on some key performance indicators when applying random packings in packed-fluidized bed reactors operating at elevated temperature was examined. Void factor is identified as a key characteristic of the packings. RMSR and Hiflow are characterized by their high void factor (>95%), while RR10, RR6 and ASB have much lower (<58%). The following conclusions are drawn:

- Packings with high void factor were found to induce limited vertical segregation of bed material. Conversely, the low packing void factor of RR6, RR10 and ASB resulted in much more noticeable segregation of bed material, especially at high gas velocities (**Paper I**).
- Packings with high void factor, with RMSR being the best example, can be added to a bubbling fluidized bed with limited effect on heat transfer, pressure drop and vertical segregation. This is a significant finding, since the ability of packings to reduce bubble size and improve gas-solid mass transfer can be expected to be significant. Packings with low void factor, with ASB being the best example, have much more significant impact on fluidization behaviour. There may be other uses for this kind of packings in fluidized beds though, that remains to be discovered (**Paper I**).
- At bed heights lower than 15 cm, beds with different packings had roughly the same fuel conversion as an ordinary bubbling bed without packings in batch CLC reactions (**Paper II**).
- For elevated bed heights (height > 15 cm), fuel conversion improved drastically when packings were used, compared to the corresponding case with no packing (**Papers II-III**). CO conversion >99.5% was achieved with bed height above 30 cm for packed-fluidized bed. With a bed height above 50 cm CO and syngas conversion was essentially 100%. This can be considered as a dramatic improvement, compared to a bubbling bed with no packings. It is believed that was due to improved gas-solid mass transfer, which was achieved by hampering of bubble growth (**Papers II-III**).
- The improvement in fuel conversion becomes even more significant if it is considered as function of oxygen carrier mass, or pressure drop over bed (**Paper II**).
- Bubble diameter in packed beds containing high void packings of RMSR and Hiflow are around 8 % less than beds without packings. Thus, the surface area where gas inter or exit the bubble decrease by 17% and the gas volume in each bubble decreases 25% (**Paper III**).

- Overall, the RMSR packing was found to provide very significant improvement in fuel conversion for all examined fuels. It also has a void factor of 0.96, meaning that it should not influence factors such as solids throughflow or pressure drop greatly. Thus, the use of this sort of packing materials to improve the performance of CLC looks promising (**Papers II-III**).
- Results indicated that the inhibition of large bubbles in the RMSR packed-fluidized bed reactor increases the mass-transfer rate (up to 9 %) and hence the fuel conversion (up to 109 %) compared to beds with no packing (**Paper III**).

5.3 Future work

By utilising different types of packings, it was tried to investigate their performance on heat and mass transfer. However, the experiments that have been done until now were in small-scale reactors with inner diameter of 78 mm. This will cause uncertainties about e.g. the influence of wall effects on the performance. Thus, the next goal for the future works, would be scaling-up a cold flow reactor with the I.D. of 220 mm and preforming experiments regarding the effect of packings on hydrodynamics and mass transfer in somewhat larger scale reactors. Also, different measurement techniques are planned to be used for the future investigations including applying pressure and humidity sensors and magnetic tracking techniques.

References

[1] O. Rueda, J. M. Mogollón, A. Tukker, and L. Scherer, "Negative-emissions technology portfolios to meet the 1.5 °C target," *Global Environmental Change*, vol. 67, p. 102238, Mar. 2021, doi: 10.1016/j.gloenvcha.2021.102238.

[2] S. Fuss *et al.*, "Betting on negative emissions," *Nature Climate Change* , vol. 4, pp. 850–853, 2014.

[3] M. , Bui *et al.*, "Carbon capture and storage (CCS): the way forward," *Energy & Environmental Science* , vol. 11, pp. 1062–1176, 2018.

[4] S. S. M. Al-Fattah *et al.*, *Carbon Capture and Storage : Technologies, Policies, Economics, and Implementation Strategies*, 1st ed. Taylor Francis Group, 2011.

[5] A. Lyngfelt and M. Rydén, "Negative CO2 Emissions with Chemical-Looping Combustion of Biomass," 2018. Accessed: Jan. 07, 2022. [Online]. Available: https://www.nordicenergy.org/wp-content/uploads/2018/07/Negative-CO2-newsletter-4-22.06.2018.pdf

[6] D. O. Kunii and Levenspiel, *Fluidization engineering*, 2nd ed. 1991.

[7] J. E. Johnsson, J. R. Grace, and J. J. Graham, "Fluidized-Bed Reactor Model Verification on a Reactor of Industrial Scale," *AIChE*, vol. 33, no. 4, pp. 619–627, 1987.

[8] C. Uraz and S. Atalay, "Oxidation of Benzene to Maleic Anhydride in a Fluidized Bed Reactor," *Chem. Eng. Technol.*, vol. 30, no. 12, pp. 1708–1715, 2007.

[9] E. J. Westerink and K. R. Westerterp, "Stable Design and Operation of Catalytic Fluidized-Bed Reactors for Multiple Reactions: Uniqueness and Multiplicity," *Chemical Engineering Science*, vol. 45, no. 1, pp. 317–332, 1990.

[10] R. A. Beck, "Evaluation of Fluid Catalyst: Development of Laboratory Scale Unit," *Industrial & Engineering Chemistry*, vol. 41, no. 6, pp. 1242–1243, 1949.

[11] J. P. Sutherland, G. Vassilatos, H. Kubota, and G. L. Osberg, "The effect of packing on a fluidized bed," *AIChE Journal*, vol. 9, no. 4, pp. 437–441, Jul. 1963, doi: 10.1002/aic.690090406.

[12] J. Aronsson, E. Krymarys, V. Stenberg, T. Mattisson, A. Lyngfelt, and M. Rydén, "Improved Gas–Solids Mass Transfer in Fluidized Beds: Confined Fluidization in Chemical-Looping Combustion," *Energy & Fuels*, vol. 33, no. 5, pp. 4442–4453, May 2019, doi: 10.1021/acs.energyfuels.9b00508.

[13] A. R. Abrahamsen and D. Geldart, "Behaviour of gas-fluidized beds of fine powders part I. Homogeneous expansion," *Powder Technology*, vol. 26, no. 1, pp. 35–46, May 1980, doi: 10.1016/0032-5910(80)85005-4.

[14] D. Geldart, "Types of gas fluidization," *Powder Technology*, vol. 7, no. 5, pp. 285–292, May 1973, doi: 10.1016/0032-5910(73)80037-3.

[15] J. R. Grace, “Contacting modes and behaviour classification of gas-solid and other two-phase suspensions,” *The Canadian Journal of Chemical Engineering*, vol. 64, no. 3, pp. 353–363, Jun. 1986, doi: 10.1002/cjce.5450640301.

[16] M. Schmitz and C. Linderholm, “Chemical looping combustion of biomass in 10- and 100-kW pilots – Analysis of conversion and lifetime using a sintered manganese ore,” *Fuel*, vol. 231, pp. 73–84, Nov. 2018, doi: 10.1016/j.fuel.2018.05.071.

[17] R. Radmanesh, J. Chaouki, and C. Guy, “Biomass gasification in a bubbling fluidized bed reactor: Experiments and modeling,” *AIChE Journal*, vol. 52, no. 12, pp. 4258–4272, Dec. 2006, doi: 10.1002/aic.11020.

[18] Y. Wang, Z. Zou, H. Li, and Q. Zhu, “A new drag model for TFM simulation of gas–solid bubbling fluidized beds with Geldart-B particles,” *Particuology*, vol. 15, pp. 151–159, Aug. 2014, doi: 10.1016/j.partic.2013.07.003.

[19] H. Wang, W. Yang, T. Dyakowski, and S. Liu, “Study of bubbling and slugging fluidized beds by simulation and ECT,” *AIChE Journal*, vol. 52, no. 9, pp. 3078–3087, Sep. 2006, doi: 10.1002/aic.10904.

[20] S. H. Hosseini, W. Zhong, M. N. Esfahany, L. Pourjafar, and S. Azizi, “CFD Simulation of the Bubbling and Slugging Gas-Solid Fluidized Beds,” *Journal of Fluids Engineering*, vol. 132, no. 4, Apr. 2010, doi: 10.1115/1.4001140.

[21] J. Ma *et al.*, “Fluidization dynamics of cohesive Geldart B particles. Part I: X-ray tomography analysis,” *Chemical Engineering Journal*, vol. 359, pp. 1024–1034, Mar. 2019, doi: 10.1016/j.cej.2018.11.082.

[22] S. Shaul, E. Rabinovich, and H. Kalman, “Typical Fluidization Characteristics for Geldart’s Classification Groups,” *Particulate Science and Technology*, vol. 32, no. 2, pp. 197–205, Mar. 2014, doi: 10.1080/02726351.2013.842624.

[23] X. Song, Z. Wang, Y. Jin, and Z. Tanaka, “Gas-solids circulating fluidization in a packed bed,” *Powder Technology*, vol. 83, no. 2, pp. 127–131, May 1995, doi: 10.1016/0032-5910(94)02948-N.

[24] J. Adanez, A. Abad, F. Garcia-Labiano, P. Gayan, and L. F. de Diego, “Progress in Chemical-Looping Combustion and Reforming technologies,” *Progress in Energy and Combustion Science*, vol. 38, no. 2, pp. 215–282, Apr. 2012, doi: 10.1016/j.pecs.2011.09.001.

[25] M. RYDEN and A. LYNGFELT, “Using steam reforming to produce hydrogen with carbon dioxide capture by chemical-looping combustion,” *International Journal of Hydrogen Energy*, vol. 31, no. 10, pp. 1271–1283, Aug. 2006, doi: 10.1016/j.ijhydene.2005.12.003.

[26] A. Abad *et al.*, “Evaluation of different strategies to improve the efficiency of coal conversion in a 50 kWth Chemical Looping combustion unit,” *Fuel*, vol. 271, p. 117514, Jul. 2020, doi: 10.1016/j.fuel.2020.117514.

[27] M. N. Khan, P. Chiesa, S. Cloete, and S. Amini, “Integration of chemical looping combustion for cost-effective CO2 capture from state-of-the-art natural gas combined

cycles," *Energy Conversion and Management: X*, vol. 7, p. 100044, Sep. 2020, doi: 10.1016/j.ecmx.2020.100044.

[28] A. Lyngfelt, A. Brink, Ø. Langørgen, T. Mattisson, M. Rydén, and C. Linderholm, "11,000 h of chemical-looping combustion operation—Where are we and where do we want to go?," *International Journal of Greenhouse Gas Control*, vol. 88, pp. 38–56, Sep. 2019, doi: 10.1016/j.ijggc.2019.05.023.

[29] J. Adánez, A. Abad, T. Mendiara, P. Gayán, L. F. de Diego, and F. García-Labiano, "Chemical looping combustion of solid fuels," *Progress in Energy and Combustion Science*, vol. 65, pp. 6–66, Mar. 2018, doi: 10.1016/j.pecs.2017.07.005.

[30] T. Mattisson *et al.*, "Chemical-looping technologies using circulating fluidized bed systems: Status of development," *Fuel Processing Technology*, vol. 172, pp. 1–12, Apr. 2018, doi: 10.1016/j.fuproc.2017.11.016.

[31] T. Berdugo Vilches, F. Lind, M. Rydén, and H. Thunman, "Experience of more than 1000 h of operation with oxygen carriers and solid biomass at large scale," *Applied Energy*, vol. 190, pp. 1174–1183, Mar. 2017, doi: 10.1016/j.apenergy.2017.01.032.

[32] C. Eder, G. Hofer, J. Beer, and T. Pröll, "Particle Mixing in Bubbling Fluidized Bed Reactors with Immersed Heat Exchangers and Continuous Particle Exchange," *Industrial & Engineering Chemistry Research*, vol. 59, no. 44, pp. 19736–19750, Nov. 2020, doi: 10.1021/acs.iecr.0c03568.

[33] R. F. Pachler, S. Penthor, K. Mayer, and H. Hofbauer, "Investigation of the fate of nitrogen in chemical looping combustion of gaseous fuels using two different oxygen carriers," *Energy*, vol. 195, p. 116926, Mar. 2020, doi: 10.1016/j.energy.2020.116926.

[34] L. Zhou, K. Deshpande, X. Zhang, and R. K. Agarwal, "Process simulation of Chemical Looping Combustion using ASPEN plus for a mixture of biomass and coal with various oxygen carriers," *Energy*, vol. 195, p. 116955, Mar. 2020, doi: 10.1016/j.energy.2020.116955.

[35] K. M. Merrett and K. J. Whitty, "Conversion of Coal in a Fluidized Bed Chemical Looping Combustion Reactor with and without Oxygen Uncoupling," *Energy & Fuels*, vol. 33, no. 2, pp. 1547–1555, Feb. 2019, doi: 10.1021/acs.energyfuels.8b03581.

[36] K. Mayer, S. Penthor, M. Stollhof, and H. Hofbauer, "Evaluation of a new DCFB reactor system for chemical looping combustion of gaseous fuels," *Applied Energy*, vol. 255, p. 113697, Dec. 2019, doi: 10.1016/j.apenergy.2019.113697.

[37] T. Chiba and H. Kobayashi, "Gas exchange between the bubble and emulsion phases in gas-solid fluidized beds," *Chemical Engineering Science*, vol. 25, no. 9, pp. 1375–1385, Sep. 1970, doi: 10.1016/0009-2509(70)85060-6.

[38] N. Nemati and M. Rydén, "Chemical-looping combustion in packed-fluidized beds: Experiments with random packings in bubbling bed," *Fuel Processing Technology*, vol. 222, p. 106978, Nov. 2021, doi: 10.1016/j.fuproc.2021.106978.

[39] J. Aronsson, D. Pallarès, and A. Lyngfelt, “Modeling and scale analysis of gaseous fuel reactors in chemical looping combustion systems,” *Particuology*, vol. 35, pp. 31–41, Dec. 2017, doi: 10.1016/j.partic.2017.02.007.

[40] J. Aronsson, D. Pallarès, M. Rydén, and A. Lyngfelt, “Increasing Gas–Solids Mass Transfer in Fluidized Beds by Application of Confined Fluidization—A Feasibility Study,” *Applied Sciences*, vol. 9, no. 4, p. 634, Feb. 2019, doi: 10.3390/app9040634.

[41] A. B. Verver and W. P. M. van Swaaij, “The heat-transfer performance of gas—solid trickle flow over a regularly stacked packing,” *Powder Technology*, vol. 45, no. 2, pp. 133–144, Jan. 1986, doi: 10.1016/0032-5910(66)80005-0.

[42] N. Nemati, P. Andersson, V. Stenberg, and M. Rydén, “Experimental Investigation of the Effect of Random Packings on Heat Transfer and Particle Segregation in Packed-Fluidized Bed,” *Industrial & Engineering Chemistry Research*, vol. 60, no. 28, pp. 10365–10375, Jul. 2021, doi: 10.1021/acs.iecr.1c01221.

[43] D. Mandal, D. Sathiyamoorthy, and M. Vinjamur, “Heat Transfer Characteristics of Lithium Titanate Particles in Gas-Solid Packed Fluidized Beds,” *Fusion Science and Technology*, vol. 62, no. 1, pp. 150–156, Aug. 2012, doi: 10.13182/FST12-A14128.

[44] A. W. M. Roes and W. P. M. van Swaaij, “Axial dispersion of gas and solid phases in a gas—solid packed column at trickle flow,” *The Chemical Engineering Journal*, vol. 18, no. 1, pp. 13–28, Jan. 1979, doi: 10.1016/0300-9467(79)80010-6.

[45] G. Donsì, G. Ferrari, and B. Formisani, “Expansion behaviour of confined fluidized beds of fine particles,” *The Canadian Journal of Chemical Engineering*, vol. 67, no. 2, pp. 185–190, Apr. 1989, doi: 10.1002/cjce.5450670204.

[46] R. Girimonte and V. Vivacqua, “The expansion process of particle beds fluidized in the voids of a packing of coarse spheres,” *Powder Technology*, vol. 213, no. 1–3, pp. 63–69, Nov. 2011, doi: 10.1016/j.powtec.2011.07.006.

[47] G. Claus, F. Vergnes, and P. le Goff, “Hydrodynamic study of gas and solid flow through a screen-packing,” *The Canadian Journal of Chemical Engineering*, vol. 54, no. 3, pp. 143–147, Jun. 1976, doi: 10.1002/cjce.5450540304.

[48] J. D. Gabor and W. J. Mecham, “Engineering Development of Fluid-Bed Fluoride Volatility Processes, Part 4. Fluidized-packed Beds: Studies of Heat Transfer, Solid gas mixing, and Elutriation,” in *AEC Research and Development Report*, 45th ed., Chemical Separation Processes for Plutonium and Uranium, 1965, pp. 1–127.

[49] E. Echigoya and G. L. Osberg, “Oxidation of ethylene using silver catalyst coated strips in an inert fluidized bed,” *The Canadian Journal of Chemical Engineering*, vol. 38, no. 4, pp. 108–112, Aug. 1960, doi: 10.1002/cjce.5450380404.

[50] A. E. McIlhinney and G. L. Osberg, “Silver sprayed cylindrical mesh packing in a fluidized bed,” *The Canadian Journal of Chemical Engineering*, vol. 42, no. 5, pp. 232–233, Oct. 1964, doi: 10.1002/cjce.5450420511.

[51] T. Ishii and G. L. Osberg, “Effect of packing on the catalytic isomerization of cyclopropane in fixed and fluidized beds,” *AIChE Journal*, vol. 11, no. 2, pp. 279–287, Mar. 1965, doi: 10.1002/aic.690110219.

[52] R. J. Farrell and E. N. Ziegler, “Kinetics and mass transfer in a fluidized packed-bed: Catalytic hydrogenation of ethylene,” *AIChE Journal*, vol. 25, no. 3, pp. 447–455, May 1979, doi: 10.1002/aic.690250309.

[53] B. Buczek and P. Zabierowski, “Confined fluidization of fines in fixed bed of coarse particles,” *Chemical and Process Engineering*, vol. 37, no. 4, pp. 545–557, Dec. 2016, doi: 10.1515/cpe-2016-0044.

[54] R. Girimonte, B. Formisani, and F. Testa, “Adsorption of CO2 on a confined fluidized bed of pelletized 13X zeolite,” *Powder Technology*, vol. 311, pp. 9–17, Apr. 2017, doi: 10.1016/j.powtec.2017.01.033.

[55] R. Girimonte, B. Formisani, and F. Testa, “CO2 adsorption in a confined fluidized bed of zeolite pellets: Influence of operating velocity,” *Particuology*, vol. 46, pp. 67–74, Oct. 2019, doi: 10.1016/j.partic.2018.08.004.

[56] J. D. Gabor and W. J. Mecham, “Radial gas mixing in fluidized-packed beds. ,” *Industrial & Engineering Chemistry Fundamentals*, vol. 3, no. 1, pp. 60–65, 1964.

[57] J. D. Gabor, “Lateral solids mixing in fludized-packed beds,” *AIChE Journal*, vol. 10, no. 3, pp. 345–350, May 1964, doi: 10.1002/aic.690100313.

[58] J. D. Gabor, “Lateral transport in a fluidized-packed bed: Part I. Solids mixing,” *AIChE Journal*, vol. 11, no. 1, pp. 127–129, Jan. 1965, doi: 10.1002/aic.690110126.

[59] J. D. Gabor, B. E. Stangeland, and W. J. Mecham, “Lateral transport in a fluidized-packed bed: Part II. Heat transfer,” *AIChE Journal*, vol. 11, no. 1, pp. 130–132, Jan. 1965, doi: 10.1002/aic.690110127.

[60] L. J. Anastasia, J. D. Gabor, and W. J. Mecham, “Engineering Development of Fluid-Bed Fluoride Volatility Processes. Part 3. Fluid-Bed Fluorination of Uranium Dioxide Fuel Pellets,” Aug. 1965.

[61] A. W. M. Roes and W. P. M. van Swaaij, “Hydrodynamic behaviour of a gas—solid counter-current packed column at trickle flow,” *The Chemical Engineering Journal*, vol. 17, no. 2, pp. 81–89, Jan. 1979, doi: 10.1016/0300-9467(79)85001-7.

[62] A. W. M. Roes and W. P. M. van Swaaij, “Mass transfer in a gas—solid packed column at trickle flow,” *The Chemical Engineering Journal*, vol. 18, no. 1, pp. 29–37, Jan. 1979, doi: 10.1016/0300-9467(79)80011-8.

[63] A. B. Verver and W. P. M. van Swaaij, “The hydrodynamic behaviour of gas—solid trickle flow over a regularly stacked packing,” *Powder Technology*, vol. 45, no. 2, pp. 119–132, Jan. 1986, doi: 10.1016/0032-5910(66)80004-9.

[64] K. R. Westerterp and M. Kuczynski, “Gas-solid trickle flow hydrodynamics in a packed column,” *Chemical Engineering Science*, vol. 42, no. 7, pp. 1539–1551, 1987, doi: 10.1016/0009-2509(87)80159-8.

[65] G. Donsì, G. Ferrari, B. Formisani, and G. Longo, “Confined fluidization of fine particles in a packed bed of coarse particles: Model and experimental description,” *Powder Technology*, vol. 61, no. 1, pp. 75–85, Apr. 1990, doi: 10.1016/0032-5910(90)80068-A.

[66] D. Ziółkowski and J. Michalski, “Onset of fluidization of fines in an organized system within voids of packings formed of spherical elements,” *Chemical Engineering Science*, vol. 47, no. 15–16, pp. 4007–4016, Oct. 1992, doi: 10.1016/0009-2509(92)85150-A.

[67] A. G. J. van der Ham, W. Prins, and W. P. M. van Swaaij, “A small-scale regularly packed circulating fluidized bed,” *Powder Technology*, vol. 79, no. 1, pp. 17–28, Apr. 1994, doi: 10.1016/0032-5910(93)02805-K.

[68] N. M. Nikačević and A. P. Duduković, “Fluid dynamics of gas-flowing solids-fixed bed contactors,” *Chemical Industry and Chemical Engineering Quarterly/CICEQ*, vol. 13, no. 3, pp. 151–162, 2007.

[69] N. M. Nikačević, Z. J. Predojević, D. Lj. Petrović, and A. Duduković, “Static holdup in Gas – Flowing solids – Fixed bed contactors,” *Powder Technology*, vol. 191, no. 1–2, pp. 122–129, Apr. 2009, doi: 10.1016/j.powtec.2008.09.011.

[70] R. Girimonte and V. Vivacqua, “Design criteria for homogeneous fluidization of Geldart’s class b solids upward through a packed bed,” *Powder Technology*, vol. 249, pp. 316–322, Nov. 2013, doi: 10.1016/j.powtec.2013.08.041.

[71] L. Davydov, W. A. Spieker, and P. Palmas, “COUNTER-CURRENT FLUIDIZED BED REACTOR FOR THE DEHYDROGENATION OF OLEFINS,” 9,150,466 B2, Oct. 06, 2015

[72] R. Girimonte, V. Vivacqua, and B. Formisani, “Extension of the model of binary fluidization to beds confined in a packing of coarse spheres,” *Powder Technology*, vol. 297, pp. 275–282, Sep. 2016, doi: 10.1016/j.powtec.2016.04.034.

[73] P. Moldenhauer, M. Rydén, T. Mattisson, A. Jamal, and A. Lyngfelt, “Chemical-looping combustion with heavy liquid fuels in a 10 kW pilot plant,” *Fuel Processing Technology*, vol. 156, pp. 124–137, Feb. 2017, doi: 10.1016/j.fuproc.2016.10.027.

[74] V. Stenberg, M. Rydén, T. Mattisson, and A. Lyngfelt, “Experimental Investigation of Oxygen Carrier Aided Combustion (OCAC) with Methane and PSA Off-Gas,” *Applied Sciences*, vol. 11, no. 1, p. 210, Dec. 2020, doi: 10.3390/app11010210.

[75] R. K. Sinnott, J.M.C., and J. F. Richardson, *Coulson & Richardson’s Chemical Engineering*, vol. 6. 2005.

[76] F. F. Incropera, T. T. Bergman, and A. Lavine, *Principles of Heat and Mass Transfer*. Singapore, 2013.

[77] J. Welty, C. Wicks, R. Wilson, and G. Rorrer, *Fundamentals of Momentum, Heat and Mass Transfer*. USA, Wiley: Hoboken, N.J., 2005.